The Journal of Physiology

Previous short-term disuse dictates muscle gene expression and physiological adaptations to subsequent resistance exercise

Martino V. Franchi[1,2], Julián Candia[3], Fabio Sarto[1], Giuseppe Sirago[1,4], Giacomo Valli[1], Matteo Paganini[1], Lisa Hartnell[3], Emiliana Giacomello[5], Luana Toniolo[1], Elena Monti[6], Leonardo Nogara[1], Tatiana Moro[1], Antonio Paoli[1], Marta Murgia[1], Lorenza Brocca[7], Maria Antonietta Pellegrino[7], Bruno Grassi[8], Roberto Bottinelli[7], Giuseppe De Vito[1], Luigi Ferrucci[3] and Marco V. Narici[1,2]

[1]*Department of Biomedical Sciences, University of Padova, Padova, Italy*
[2]*CIR-MYO Myology Center, University of Padova, Padova, Italy*
[3]*National Institute on Aging, Baltimore, Maryland, USA*
[4]*Institute of Sport Sciences and Department of Biomedical Sciences, University of Lausanne, Lausanne, Switzerland*
[5]*Department of Medicine, Surgery and Health Sciences, University of Trieste, Trieste, Italy*
[6]*Baxter Laboratory for Stem Cell Biology, Department of Microbiology and Immunology, Stanford University, Stanford, California, USA*
[7]*Department of Molecular Medicine, Institute of Physiology, University of Pavia, Pavia, Italy*
[8]*Department of Medicine, University of Udine, Udine, Italy*

Handling Editors: Karyn Hamilton & Mark Viggars

The peer review history is available in the Supporting information section of this article (https://doi.org/10.1113/JP287003#support-information-section).

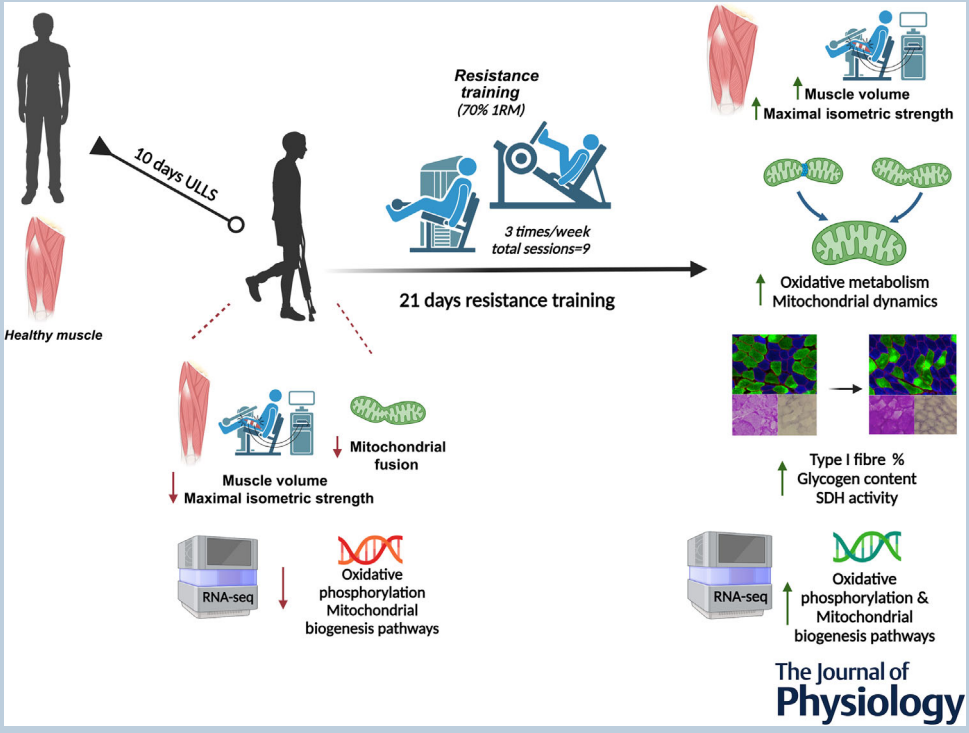

Abstract figure legend Eleven young healthy males underwent 10 days of unilateral lower limb suspension (ULLS) followed by a 21 day period of active recovery (AR) using resistance exercise performed three times a week at 70% of the one repetition maximum (1RM), equating to a total of nine training sessions. At baseline, immediately after ULLS,

DOI: 10.1113/JP287003

and 3 days after the last training session of the AR period, we assessed maximal isometric muscle force production by dynamometry, and we estimated muscle volume through panoramic ultrasound techniques. Vastus lateralis biopsies were collected at the same time points. After 10 days of ULLS, we observed decreased muscle force and volume, accompanied by reductions in proteins related to mitochondrial fusion and downregulation of the expressions of gene pathways related to oxidative phosphorylation, fatty acid metabolism and mitochondrial biogenesis. After only nine sessions of resistance exercise, muscle force was restored and muscle volume was markedly increased (even exceeding baseline values); however, most of the molecular and gene expression findings pointed towards a marked regulation of oxidative phenotype and metabolism in contrast with what is usually observed in response to resistance exercise.

Abstract Short-term unloading experienced following injury or hospitalisation induces muscle atrophy and weakness. The effects of exercise following unloading have been scarcely investigated. We investigated the functional and molecular adaptations to a resistance training (RT) programme following short-term unloading. Eleven males (22.09 $\pm$ 2.91 years) underwent 10 days of unilateral lower limb suspension (ULLS) followed by 21 days of knee extensor RT (three times/week). Data collection occurred at Baseline (LS0), after ULLS (LS10) and at active recovery (AR21). Knee extensor maximum voluntary contraction (MVC) was evaluated. Quadriceps volume was estimated by ultrasonography. Muscle fibre cross-sectional area, fibre type distribution, glycogen content and succinate dehydrogenase (SDH) activity were measured from vastus lateralis biopsies. Mitochondrial-related proteins were quantified by western blot and transcriptional responses were assessed by RNA sequencing. Following ULLS, quadriceps volume and MVC decreased significantly (3.7%, $P < 0.05$; 29.3%, $P < 0.001$). At AR21 (*vs*. LS10), MVC was fully restored (42%) and quadriceps volume increased markedly (18.6%, $P < 0.001$). Glycogen content and whole-body water increased at AR21 (14%, $P < 0.001$; 3.1%, $P < 0.05$). We observed a marked increase in fibre type I at AR21 (38%, $P < 0.05$). SDH immunoreactivity increased significantly after exercise (20%, $P < 0.001$). Mitochondrial fusion (MFN1, MFN2 and OPA1) and fission (DRP1) proteins were markedly increased by RT, and the most differentially expressed genes belonged to oxidative phosphorylation pathways. In contrast with what is usually observed after RT, oxidative metabolism, slow fibre type and mitochondrial dynamics were enhanced beyond expected. We propose that prior exposure to short-term muscle unloading may drive the nature of molecular adaptations to subsequent RT.

(Received 30 May 2024; accepted after revision 18 December 2024; first published online 10 January 2025)
Corresponding author M. V. Franchi: Human Neuromuscular Physiology Lab, Department of Biomedical Sciences, University of Padova, Padova, Via Marzolo 3, 35131, Italy. Email: martino.franchi@unipd.it

Key points

- Short-term unloading is often experienced during recovery from injuries and hospitalisation, leading to loss of muscle mass and strength.
- Although exercise can be beneficial in mitigating/reversing such alterations during disuse, only a few studies have focused on the effects of exercise following muscle unloading.
- With an integrative physiological approach, we aimed to elucidate the basic mechanisms of muscle function recovery in response to 21 days of resistance exercise that followed 10 days of unilateral lower limb suspension (ULLS), assessing whether the mechanisms underlying recovery are defined by a specific reversal of those that occurred during disuse.
- Resistance training was successful in recovering functional and structural muscle properties after 10 days of ULLS, but in contrast with what is usually observed in response to this training modality, oxidative metabolism and slow fibre type were mostly enhanced.
- We propose that prior exposure to short-term muscle unloading may drive the adaptations to subsequent exercise.

Introduction

The full or partial absence of mechanical loading experienced during periods of physical inactivity leads to progressive and inexorable loss of muscle mass, strength and power (Nunes et al., 2022; Preobrazenski et al., 2023), coupled with impairment of oxidative metabolism and insulin sensitivity (Booth et al., 2017; Narici et al., 2020; Shur et al., 2022). A significant reduction of muscle cross-sectional area (CSA) has been detected as early as 2 days after knee bracing (∼2%) (Kilroe et al., 2020), progressing to ∼4–10% after 10–23 days of either bed rest or unilateral lower limb suspension (ULLS) (de Boer et al., 2007; Kubo et al., 2004; Monti et al., 2021; Sarto et al., 2022). The loss of muscle strength typically exceeds that of muscle mass, ranging from ∼9% after 5 days of limb immobilisation (Wall et al., 2013) to ∼14% after 10–14 days of bed rest or limb suspension (de Boer et al., 2007; Monti et al., 2021). Hence, even short-term periods of muscle unloading (∼7–10 days), commonly experienced during recovery from injuries and hospitalisation (Mikines et al., 1991; Shur et al., 2022), could induce sizeable muscle atrophy and weakness (Atherton et al., 2016; Monti et al., 2021; Sarto et al., 2022).

Although physical activity and exercise are commonly used to speed up recovery from these impairments (Oikawa et al., 2019), the literature concerning the mechanisms of neuromuscular function recovery strategies is scarce, and only a few studies have investigated the effects of exercise countermeasures following periods of muscle unloading. These studies employed limb immobilisation or suspension and showed full recovery of muscle mass, strength and fibre-specific force after 3–4 weeks of resistance training (RT) (Brocca et al., 2015; Campbell et al., 2013; Elam et al., 2022; Sarto et al., 2022; Suetta et al., 2009). However, it is still not established what modality of exercise induces the fastest and most complete recovery of physiological functions and muscle metabolism. Moreover, it has also been argued that the molecular phenomena underlying the recovery phase are not simply a reversal of those occurring in the disuse phase (Booth et al., 2017; Stein & Bolster, 2006).

In the pioneering 'Dallas Bed Rest study', Saltin et al. (1968) showed that maximal oxygen uptake was markedly impaired by 20 days of bed rest, but was fully recovered and even became greater than pre-bed rest after 60 days of endurance exercise (running). The study highlighted that a reduction in $\dot{V}_{O_2max}$ represents another signature of muscle disuse, which is often accompanied by suppression of mitochondrial bioenergetics genes, decreased mitochondrial content, increased reactive oxygen species production and decreased insulin sensitivity (Abadi et al., 2009; Alibegovic et al., 2010; Dirks et al., 2020; Dulac et al., 2024; Mikines et al., 1991; Stuart et al., 1988; Zuccarelli et al., 2021). Because during inactivity the loss of muscle power, strength and mass can occur earlier and at greater rates than the loss of mitochondrial mass and function (Marshall et al., 2022; Pileggi et al., 2023; Zuccarelli et al., 2021), scientists and practitioners may tend to favour resistance exercise, over aerobic training, as an ideal recovery strategy. Interestingly, a previous study showed that 12 weeks of high-intensity RT following 3 weeks of knee immobilisation led to an increase in type I fibres (Hortobágyi et al., 2000). This finding was unexpected since RT alone (without a prior period of disuse) has not been associated with such an effect (Folland & Williams, 2007; Komi et al., 2003). This prompts the question of whether the effects of exercise on muscle physiological adaptations can be influenced by the previous level of activity/inactivity.

Based on these premises, we aimed to elucidate the basic mechanisms of muscle function recovery in response to resistance exercise following 10 days of ULLS, aiming to assess whether the phenomena underlying recovery were a specular reversal of those that occurred during disuse. Beyond the *in vivo* assessment of muscle mass and strength changes, we investigated the molecular adaptations of human skeletal muscle after 3 weeks of RT, exploiting a transcriptional profiling approach to assess changes in pathways related to muscle hypertrophy and metabolism. We hypothesised that resistance exercise would lead to full recovery of muscle function, mass and structure through an efficient counteraction of the molecular regulators of muscle disuse atrophy, mostly related to the promotion of muscle hypertrophy, consistent with the exercise modality employed.

Martino Franchi received his PhD from the Manchester Metropolitan University investigating human muscle functional, structural and molecular remodelling to lengthening *vs.* shortening contraction. In 2013, he joined the MRC/ARUK Centre for Musculoskeletal Ageing Research at the University of Nottingham as a postdoctoral fellow investigating muscle and tendon adaptations to eccentric and plyometric exercise in ageing populations. Between 2017 and 2019, he was appointed as a research fellow (with double affiliation) in muscle plasticity, working on muscle mechano-transduction, and in the Sports Medicine Research Group at the Balgrist University Hospital (University of Zürich, Switzerland). He is now an Assistant Professor (with tenure track) in Human Physiology at the Department of Biomedical Sciences of the University of Padova in Italy. His main interests lie in muscle functional and structural adaptations to loading, disuse and ageing, with a 'from-the-macro-to-the-micro' approach.

Table 1. Generalities and characteristics of the volunteers (*N* = 11)

ID	Age (years)	Height (m)	Weight (kg)	BMI (kg m^{-2})
S1	22	1.79	68.25	21.30
S2	23	1.78	72.31	22.82
S3	21	1.77	84.30	26.91
S4	20	1.80	70.75	21.84
S5	28	1.82	70.96	21.42
S6	19	1.72	61.39	20.75
S7	21	1.77	81.77	26.10
S8	24	1.80	73.12	22.57
S9	20	1.75	64.97	21.09
S10	19	1.73	66.93	22.36
S11	26	1.80	79.17	24.44
Mean	**22.09**	**1.78**	**72.17**	**22.87**
SD	**2.91**	**0.03**	**7.10**	**2.07**

Methods

Volunteers

Twelve healthy and recreationally active young males were recruited. One volunteer dropped out before starting the lower limb suspension period for personal reasons. Two other volunteers decided not to undergo muscle biopsy procedures after the active recovery (AR) period for personal reasons. Thus, the data presented are pooled from a total of 11 young participants (22.1 ± 2.9 years, body mass index 22.9 ± 2.1 kg m^{-2}; see Table 1 for all subject characteristics); for the molecular-related data only, *N* was 11 for baseline and post-limb suspension time points and *N* was 9 for the data acquired after the AR period [unless specified as for Periodic acid Schiff (PAS) and succinate dehydrogenase (SDH) staining where *N* was 9 for all time points]. The maximum voluntary contraction (MVC) data have already been published in a previous paper from our lab (Sarto et al., 2022) focused on electrophysiological data obtained in the same ULLS campaign. Similarly, for clarity purposes, ultrasound data that have been partially published in Sarto et al. (2022) (muscle CSAs) have been used for the estimation of muscle volume shown in the present paper.

Only male individuals were included as the ULLS model can be associated with an increased risk for deep venous thrombosis (DVT), which is generally more common in females (Bleeker et al., 2004; Roach et al., 2014). The sample size was defined with *a priori* power analysis calculation (see statistical analysis section).

The inclusion criteria were as follows: age between 18 and 35 years, body mass index between 20 and 28 kg m^{-2} and involvement in recreational physical activities (one to three times per week). The exclusion criteria were defined to exclude sedentary individuals, professional athletes, smokers, or anyone with a history of DVT, acute or chronic musculoskeletal, metabolic or cardiovascular disorders. Evaluation of physical activity levels was carried out via the Global Physical Activity Questionnaire (GPAQ) at baseline and then after ULLS (LS10) and at active recovery (AR21) time points (see the Supporting Information).

Ethical approval

Participants were informed about all the experimental procedures through an interview and a volunteer information sheet. Volunteers signed a written consent form and were granted the opportunity to drop out of the study at any stage. The study conformed to the standards set by the latest revision of the *Declaration of Helsinki*, except for registration in a database, and the study was approved by the local ethics committee of the Department of Biomedical Sciences of the University of Padova (reference number HEC-DSB/01-18).

Study design

The protocol consisted of 1 day of familiarisation that occurred before the real experimental procedures took place at baseline (LS0), after 10 days of limb suspension (LS10) and 21 days of AR based on resistance exercise (AR21) (see next sub-section for details), as presented in Sarto et al. (2022). All experimental measurements (including muscle biopsies) were performed again after the AR period, specifically 3 days after the last training session of the AR phase, to avoid potential muscle fatigue. Participants were asked to refrain from caffeine and alcohol consumption and any form of exercise in the 24 h preceding the data collection at each time point. Further, they were asked to maintain their habitual diet period throughout the entire study (see dietary monitoring section). Volunteers were tested at the same time of the day on each testing day to minimise influences of circadian pattern change. A summary sketch of the study design is provided (Fig. 1).

A ULLS model (Berg et al., 1991) was employed for 10 consecutive days. As described in Sarto et al. (2022), each volunteer was provided with a shoe presenting an elevated sole (50 mm) for the non-dominant leg, while the dominant leg (i.e. the intervention leg) was suspended and kept at a slightly flexed position (∼15/20 degrees of knee flexion) using straps specifically tailored for this purpose. Volunteers were instructed to walk on crutches during the whole intervention period and to strictly refrain from loading the suspended leg. A familiarisation session for the participants was carried out, so they could practise their daily tasks during limb suspension (Tesch et al., 2016). Volunteers were instructed to wear

elastic compression socks on the suspended leg during the 10 days of ULLS and daily to perform passive, range of motion, non-weight-bearing exercises of the ankle as a precaution to prevent DVT (Bleeker et al., 2004). An ultrasound-Doppler examination was performed after 5 days of ULLS to exclude severe risks. Compliance of the participants was evaluated through daily calls and by comparing triceps surae circumference and local skin temperature after 5 and 10 days of ULLS, as suggested by Tesch et al. (2016).

Active recovery protocol

After 10 days of limb suspension, volunteers were enrolled in a 21 day AR programme based on resistance exercise. The training phase started 3 days after the LS10 measurements to grant recovery from the potential damage and discomfort induced by the muscle biopsy collection. Volunteers trained three times per week: the usual weekly training scheme was to train every other day, and when not possible the training sessions were separated by at least 24 h. The AR programme consisted of three sets of 10 repetitions of unilateral leg press and leg extension exercises performed at 70% of one-repetition maximum (1RM). Both exercises were executed from full knee extension (0 degrees) to ∼90 degree limb flexion. 1RM was indirectly estimated since the volunteers had just undergone 10 days of unloading. Briefly, 4–6RM (i.e. the heaviest load that they could lift and lower under control in the range between four and six repetitions) was assessed and 1RM was subsequently estimated using the formula of Brzycki (1993), with values lying within the ranges indicated by the National Strength and Conditioning Association (NSCA) training load chart (Beachle & Earle, 1994). 1RM was estimated within a maximum of five attempts and was therefore reassessed at the first training session of each week, so the training load could be adjusted accordingly. Each session was supervised by an expert trainer with a university degree in Sports Science and preceded by a standardised warm-up consisting of 10 bodyweight squats and two leg-press sets of 10 repetitions at 30% 1RM. Sets were separated by 2 min of rest. The time under tension was set at ∼2 s, in both the concentric and eccentric phase, and a metronome was employed during all the sessions. At the end of each training session, a rating of perceived exertion (RPE) score and muscle soreness were collected. RPE was evaluated with the CR10-scale (0 = rest; 10 = maximal) (Foster et al., 1995), and muscle soreness with a modified CR10-scale as previously described (Cook et al., 1997; Franchi et al., 2019), where

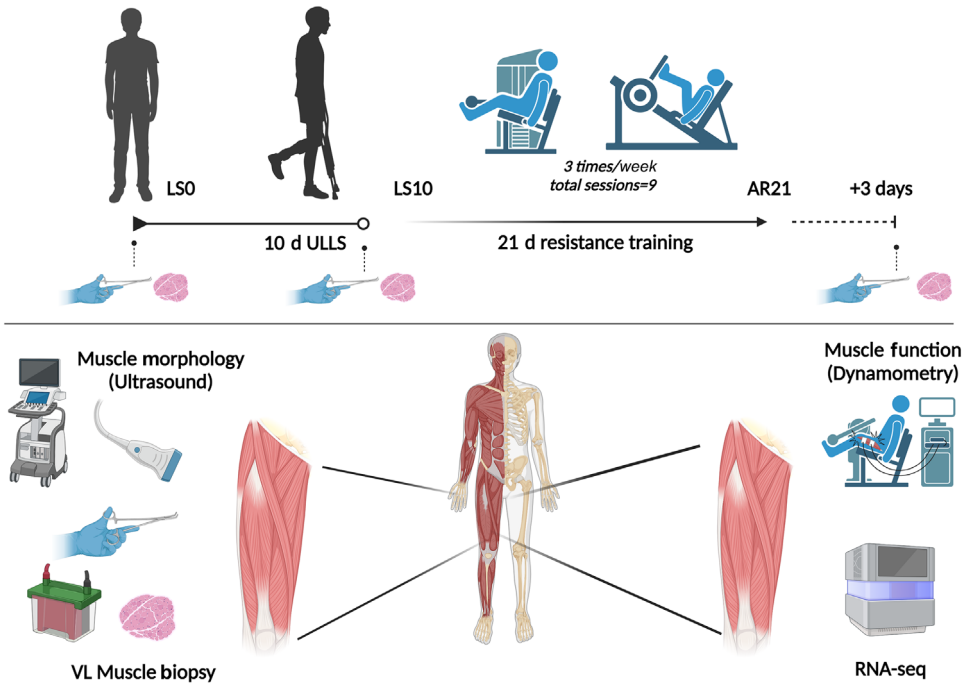

Figure 1. Sketch of the study design
Volunteers underwent a unilateral lower limb suspension period of 10 days followed by 21 days of active recovery by means of nine total sessions of resistance training. Data collection was performed on the right leg at baseline (LS0), at the end of limb suspension (LS10) and 3 days after the end of the exercise recovery period (AR21). Quadriceps muscle volume and vastus lateralis (VL) muscle architecture were assessed by ultrasonography, whereas muscle function was assessed by muscle dynamometry by calculating the isometric maximum voluntary contraction (MVC). VL muscle biopsies were collected for histological and immunofluorescence assessments, as well as for western blotting and RNA sequencing.

'0' represented 'no soreness' and 10 corresponded to 'the most muscle soreness they could bear'. The total and weekly training volume was calculated as the product of the total repetitions performed and the training load in kilograms (Schoenfeld et al., 2019).

The duration of the AR period (i.e. 21 days, compared to the 10 days of ULLS) was decided based on the fact that full muscle function restoration has been observed following a retraining period that lasted twice as long as the disuse phase (Suetta et al., 2009). In their study, the AR period consisted of 4 weeks following 2 weeks of lower limb immobilisation (Suetta et al., 2009). Since our purpose was to achieve full recovery of muscle strength, MVC was evaluated after 10 days of AR to monitor the level of muscle function restoration with respect to baseline values (Sarto et al., 2022).

Muscle morphology, architecture and function

Muscle CSA and volume. Quadriceps femoris (QF) and vastus lateralis (VL) CSA were evaluated using extended-field-of-view (EFOV) (i.e. panoramic) ultrasonography. A 47 mm, 7.5 MHz linear array transducer (Mylab70, Esaote, Genoa, Italy) was used to collect transversal images as previously described by our research group for several studies (Franchi, Badiali et al., 2022; Franchi, Sarto et al., 2022; Monti et al., 2020; Quinlan et al., 2021). In brief, different regions of interest were identified at 20, 30, 40, 50, 60 and 70% of the femur length (measured from the greater trochanter to the mid-patellar point) and marked on the skin, considering the mid-patellar point as the beginning of the QF and VL muscles (0%), and the great trochanter landmark as their end (100%). The probe was positioned transversally on the medial portion of the leg, thus starting the acquisition from the medial borders of the vastus medialis. The transducer was then moved along the transverse plane, and it was stopped after visualising the lateral borders of the VL. An adjustable guide was used in each acquisition to keep the same transverse path (Quinlan et al., 2021). Care was taken to keep as constant as possible both pressure during all the image acquisition and acquisition velocity throughout the different testing sessions, and enough transmission gel was applied to improve the acoustic contact.

QF and VL CSA measures were then obtained by tracing the contours of the quadriceps and VL using ImageJ software (1.52v; National Institutes of Health, Bethesda, MD, USA). VL and QF volume were then estimated by using the truncated cone formula, as previously reported (Monti et al., 2020; Quinlan et al., 2021; Sarto et al., 2021; Tracy et al., 2003). Partial muscle volume was calculated from 20 to 70% of the femur length of each volunteer using the CSA data obtained from panoramic ultrasound scans. As no scans were performed below 20% and above 70%, the remaining CSA values for the 10, 80 and 90% axials were estimated by fitting a spline curve (third-order polynomial) through the CSA values that were physically measured, as previously done by Seynnes et al. (2008). The values corresponding to 0%and 100% of femur length were set as 0 (Monti et al., 2020). Muscle volume was then assumed to approximate muscle mass since muscle density is 1.0597 g/cm^3 (Mendez & Keys, 1960). QF and VL volume were calculated as the sum of the calculated volume between each measured (20–70%) or estimated (10, 80–90%) CSA.

Muscle architecture. Muscle architecture of the VL muscle was measured *in vivo* using B-mode ultrasonography (Mylab70, Esaote). Ultrasound images were obtained on the right leg at 50% of the femur length with the participant lying in the supine position. After the medial and lateral borders of the VL were identified (Franchi et al., 2014), 50% of the distance between the VL borders was chosen for image acquisition. VL fascicle length (Lf) and pennation angle (PA) were measured using a 47 mm, 7.5 MHz linear-array probe as described (Franchi et al., 2015): the probe was positioned over the belly of the VL, carefully adjusted to the fascicle plane while minimal pressure was applied. Two ultrasound scans were then analysed using ImageJ image analysis software (Image J, NIH). Briefly, fascicles were digitised using the segmented line tool following the fascicle pathway and curvature within their visible portion. Then, fascicle length was determined through manual extrapolation (i.e. straight-line tool used) of fibres and aponeuroses if a portion of the fascicle extended outside of the captured ultrasound image. Usually, two to three fascicles were evaluated for each scan, and their average value was taken as the final Lf value. PA was measured at the intersection between the fascicles and the deep aponeurosis. An average of at least three PA measures per image was performed (Franchi et al., 2018).

Knee-extensor muscle force. *In vivo* muscle function assessment has been previously described for this cohort by our group (Sarto et al., 2022), and thus the data related to the knee extensor MVC have been previously published. MVC was evaluated at baseline, LS10 and AR21 in an isometric fashion and at 90 degrees of knee flexion using a custom-made dynamometer. Volunteers were instructed to push as strongly and as fast as they could and to try to maintain their maximal force output for ∼4 s. Visual feedback and vocal encouragement were provided. Three trials were recorded, separated by 1 min of rest. The force signal was sampled at 1000 Hz using Labchart software (v.8.13, AD Instruments, Colorado Springs, CO, USA). The maximum force value reached during the three trials was considered as the MVC value.

Body water content, lean mass and dietary monitoring

Dual-energy X-ray absorptiometry. Body composition was assessed by dual-energy X-ray absorptiometry (DEXA; Horizon Wi, TECHNOLOGIC S.r.l. 'Hologic Italia'). Before the analysis participants were asked to remove all metal objects; they were then positioned supine with upper and lower limbs properly abducted for the analysis. Outputs of bone mineral content and density, fat and lean mass were obtained.

Bioelectrical impedance analysis. Body composition assessment was obtained via bioelectrical impedance analysis (BIA) using a single frequency of a 50 kHz device (BIA 101 BIVA®PRO, Akern Systems, Florence, Italy). Participants were positioned in a supine position with legs and shoulders respectively abducted at 45and 30 deghrees for 3–5 min before the measurements. Values of resistance (R) and reactance (Xc) were obtained by placing the electrodes on the right side of the body and used to estimate lean mass, fat mass, intra- and extracellular water, and total water. Four low intrinsic impedance adhesive electrodes (Biatrodes Akern Srl, Florence, Italy) were placed on the back of the hands and the other four electrodes on the neck of the corresponding feet.

Dietary monitoring. During the first week after recruitment, and then again during ULLS and AR, participants were asked to complete a 3 day food diary which was analysed using nutritional software (Dieta Ragionata 7.0). Volunteers were instructed to describe their meals (including drinks) choosing two regular weekdays and one weekend day. From the food diaries, individual daily dietary and macro-nutrient intake was estimated as the average of the 3 days.

Muscle biopsies

VL muscle biopsies were collected ∼2 cm from the central motor point (Aubertin-Leheudre et al., 2020), as described in Sarto et al. (2022). Between the three biopsy sampling sessions, an ∼2 to 3 cm distance was maintained to avoid any effects of prior sampling, and thus the biopsies were collected ∼2 cm proximally from the central motor point (LS0 biopsy), then ∼2 cm above (LS10 biopsy) and ∼2 cm below (AR21 biopsy) the central motor point (Sarto et al., 2022). All biopsies were collected in resting conditions, so no exercise sessions had previously occurred. An AR21 biopsy was collected 3 days after the last training session of the AR phase.

Muscle biopsies were obtained by adopting the conchotome technique (Dietrichson et al., 1987) using conchotome forceps (Gebrüder Zepf Medizintechnik GmbH & Co. KG, Dürbheim, Germany). In brief, 2 ml of lidocaine (2%) was injected into the sampling area, and a small incision of muscle and fascia was performed. Muscle samples were divided into different parts as follows: (i) a part for mRNA analysis, which was frozen in liquid nitrogen and stored at −80°C; (ii) a part for immunohistochemical analysis, which was frozen in isopentane, cooled down on liquid nitrogen and stored at −80°C; and (iii) a final part for western blotting and biochemical analyses, which was washed in ice-cold saline solution, then frozen in liquid nitrogen and stored in air-tight cryotubes at −80°C.

Muscle fibre analyses

Immunofluorescence. Muscle sections were obtained from frozen samples and stored for several analyses, including assessment of fibre type composition, fibre morphology and staining for specific targets.

Frozen samples were cut using a manual cryostat (Leica CM1850, Wetzlar, Germany), producing 10 µm thick sections. Sections were stained with anti-MYH antibodies to reveal fibre types, using monoclonal antibodies BA-D5 and SC-71, which were originally described by Schiaffino et al. (1989), and 6H1, originally described by Lucas et al. (2000). These three antibodies, which are distributed by Developmental Studies Hybridoma Bank (DSHB), were applied together using appropriate secondary antibodies, as previously described (Murgia et al., 2017). In addition, we used monoclonal antibody BF-35, also distributed by DSHB, which is reactive with MYH7 and MYH2 but not with MYH1, thus staining all fibre types, except pure type 2X fibres, both in rat (Schiaffino et al., 1989) and human muscles (Smerdu et al., 1994). Fibre profiles were revealed by far-red Wheat Germ Agglutinin (WGA) staining (Thermo Fisher, W32466, Waltham, MA, USA). Sections were examined with a Leica DM6B microscope, equipped with a DFC 7000T camera. Pictures were analysed using FIJI software (Schindelin et al., 2012), obtaining measurements of fibre CSA and myosin isoform identification (all available fibres were measured, ∼200–300 fibres per section).

Periodic acid Schiff staining. Specimens were processed following the manufacturer protocol (Merck, Darmstadt, Germany). Briefly, frozen sections were rapidly rinsed in running tap water and immersed in 0.5% periodic acid for 10 min, rinsed in running tap water and incubated for 15 min in Schiff reagent (Merck). Specimens were washed three times in a sulphurous solution containing 0.5% potassium metabisulphite and 0.05 M hydrochloric acid, washed for 3 min in tap water, rinsed in distilled water, dehydrated and mounted with a resinous mounting medium. Images were acquired with a Leica DM500

microscope (Leica) equipped with a Leica ICC50 digital camera (Leica). Images were converted to greyscale with Fiji free software to measure the intensity of PAS staining. The staining was evaluated by measuring the mean grey intensity of multiple regions outlined inside the fibres (Fernandez et al., 1995).

Succinate dehydrogenase staining. Frozen sections were incubated for 60 min in a solution containing 0.2 M sodium succinate, 1 mg ml^{-1} Nitro Blue Tetrazolium (Sigma Aldrich, Milan, Italy) in 0.2 M Tris-HCl buffer, pH 7.4. The enzymatic reaction was stopped by dipping the slides in water. Specimens were air-dried in the dark and mounted in gelatin-glycerol. Images were acquired with a Leica DM500 microscope (Leica) equipped with a Leica ICC50 digital camera (Leica). SDH activity was calculated with Fiji software by converting images to greyscale and measuring the mean grey intensity values of each fibre as previously described (Giacomello et al., 2020).

SDS-PAGE and western blotting analyses

SDS-Page determination of myosin heavy chain isoform distribution. A portion of muscle tissue was stored in a skinning solution at −20°C. For total myosin heavy chain (MyHC) protein quantification, a portion of fibres was solubilised directly in Laemmli solution (62.5 mM Tris-HCl pH 6.8, 2.3% SDS, 10% glycerol) (Laemmli, 1970), in the presence of protease and phosphatase inhibitors, and treated with one cycle of thermal shock from +65°C to −20°C to allow complete protein resuspension. Protein concentration was determined by the Folin–Lowry method, using BSA as a reference (Lowry et al., 1951). Approximately 10 µg of extract was separated onto 8% SDS-PAGE mini-gels (Mini-PROTEAN Tetra Handcast System, Bio-Rad, Hercules, CA, USA) for 1 h at 50 V (constant voltage) and then for ∼40 h at 60 V (constant voltage), in a cold room. Following electrophoresis, the gel was stained using modified Colloidal Coomassie Blue Staining (Kang et al., 2002; Neuhoff et al., 1988). The protein bands (MyHC-1, MyHC-2A and MyHC-2X) were then quantified by densitometric analysis to assess the relative percentage proportion in each participant.

Western blot analyses: mitochondrial protein content. Frozen muscles were pulverised in a steel mortar using a ceramic pestle, with the constant addition of liquid nitrogen to maintain muscle component properties. The powder thus obtained was homogenised with lysis buffer containing 20 mM Tris-HCl, 1% Triton X-100, 10% glycerol, 150 mM NaCl, 5 mM EDTA, 100 mM NaF and 2 mM NaPPi (tetra-sodium pyrophosphate) supplemented with 5× protease inhibitor, 1× phosphatase inhibitors (Protease Inhibitor Cocktail, Sigma-Aldrich) and 1 mM PMSF. The homogenate obtained was centrifuged at 22413 RCF or *g* force for 20 min at 4°C, and protein quantification was performed using the RC-DC™ (reducing agent and detergent compatible) protein assay (Bio-Rad). Forty micrograms of lysates was denatured at 95°C for 5 min and loaded on a 4–20% gradient Precast gel (Bio-Rad). An electrophoretic run was carried out at constant current (100 V) for about 2 h in a running buffer at pH 8.8 (25 mM Tris, 192 mM glycine, 1% SDS, Bio-Rad) and the proteins were then transferred (blotting) to a PVDF membrane activated with methanol. The transfer was carried out at constant voltage at 100 V for 2 h at 4°C or at constant 35 mA overnight (O/N) in a cold transfer buffer containing 25 mM Tris, 192 mM glycine and 20% methanol. Effective protein transfer to the membrane was verified by staining with Ponceau S (Merck, Darmstadt, Germany) red staining in acetic acid (0.2% Ponceau S in 3% acetic acid) for 15 min under gentle shaking at room temperature, followed by washes to remove the excess and clear the membrane.

To minimise the background, non-specific binding sites present on the PVDF membrane were saturated with a blocking solution consisting of 5% fat-free milk in 1× TTBS (0.02 M Tris, 0.05 M NaCl and 0.1% Tween-20) for 2 h at room temperature with constant shaking. Ultimately, the membrane was washed with 1× TTBS and incubated O/N at 4°C with the specific primary antibody appropriately diluted in a solution of 1× TTBS containing 5% BSA or 5% fat-free milk (see below). Subsequently, the membrane was washed in 1× TTBS and incubated for 1 h at room temperature in constant agitation, with a secondary antibody diluted suitably as previously referred to for the primary antibodies. Protein detection was made using the Amersham ECL Select™ detection system (Cytiva Life Sciences, ex GE Healthcare, Piscataway, NJ, USA) which highlights the HPR substrate by a chemiluminescent reaction. The membrane was gained through the analysis software ImageQuant™ LAS 4000 (GE Healthcare Life Sciences), and the exposure time was adjusted in an automatic manner or editable depending on the intensity of the emitted signal. The inverted bands present on the scanned images were quantified with Adobe Photoshop, and a BAP value (Brightness Area Product), given by the product of the brightness and the area of the band itself, was defined. Target protein levels were normalised to total proteins in lysates by Ponceau staining or evaluated between phosphorylated and unphosphorylated total forms of the same protein.

The primary antibodies used in this work were: Rabbit polyclonal anti TOM20 (1:1000, FL-145, # sc-11415, Santa Cruz Biotechnology, Santa Cruz, CA, USA); Rabbit polyclonal anti PGC-1alpha (1:1000, ab54481, Abcam, Cambridge, MA, USA); Mouse monoclonal anti MFN1

(1:1000, ab57602, Abcam); Rabbit polyclonal anti MFN2 (1:1000, ab50843, Abcam); Mouse monoclonal anti OPA1 (1:3000, ab119685, Abcam); Rabbit polyclonal anti p-DRP1(ser616) (1:1000, #3455, Cell Signaling, Danvers, MA, USA); Rabbit polyclonal anti p-DRP1(ser637) (1:1000, #4867, Cell Signaling); Rabbit monoclonal anti DRP1 (1:3000, #8570, Cell Signaling); Rabbit polyclonal anti FIS1 (1:1000, ab71498, Abcam).; Mouse Antibody cocktail Total OXPHOS (1:1000, ab110411, Abcam); The secondary antibodies used were Rabbit anti-mouse IgG (1:5000 or 1:10,000, P0260, Dako, Carpinteria, CA, USA) and Goat anti-rabbit IgG (1:10000, #7074S, Cell Signaling).

RNA extraction, sequencing and transcriptomic analysis

RNA sequencing (RNA-seq) was performed to investigate changes in mRNA transcript abundances that occurred during the 10 days of muscle disuse and subsequent AR. We decided to investigate the expression of genes involved in adaptations to exercise. RNA was extracted from muscle tissue samples by REPROCELL (USA) using a Norgen Animal Tissue RNA Purification Kit #257 (Norgen Biotek Corp., Ontario, Canada). RNA-seq was performed at the Frederick National Laboratory for Cancer Research Sequencing Facility, NIH. The libraries were made using the TruSeq Stranded Total RNA Library Prep protocol from Illumina. This protocol involves the removal of rRNA using biotinylated, target-specific oligos combined with Ribo-Zero rRNA removal beads. The RNA was fragmented into pieces, and the cleaved RNA fragments were copied into first-strand cDNA using reverse transcriptase and random primers, followed by second-strand cDNA synthesis using DNA Polymerase I and RNase H. The resulting double-strand cDNA was used as the input to a standard Illumina library prep with end-repair, adapter ligation and PCR amplification performed to provide a library ready for sequencing. Samples were sequenced on a NovaSeq 6000 on an S4 flowcell using paired-end sequencing with a read length of 150 bp. The sequencing quality of the reads was assessed using FastQC (v.0.11.5; https://www.bioinformatics.babraham.ac.uk/projects/fastqc/), Preseq (v.2.0.3) (Daley & Smith, 2013), Picard tools (v.2.17.11; https://broadinstitute.github.io/picard/) and RSeQC (v.2.6.4) (Wang et al., 2012). The samples had 295–419 million pass filter reads with more than 90% of bases above the quality score of Q30. In addition, Kraken (v.1.1) (Wood & Salzberg, 2014) was used as a quality-control step to assess microbial taxonomic composition. Reads were trimmed using Cutadapt (v.1.18) (Martin, 2011) to remove sequencing adapters prior to mapping to the human reference genome hg38 using STAR (v.2.7.0f) (Dobin et al., 2013) in two-pass mode. Expression levels were quantified using RSEM (v.1.3.0) (Li & Dewey, 2011) with GENCODE annotation (v.21) (Harrow et al., 2012). In order to filter out low expression genes, filterByExpr() from the package edgeR (v.3.32.1) (Robinson et al., 2010) was used, followed by quantile normalisation using the voom algorithm (Law et al., 2014) from the Limma R package (v.3.46.0) (Smyth, 2004), and empirical Bayes smoothing of standard errors to assess differentially expressed genes adjusted for subject ID (paired analysis) between time points (LS0, LS10, AR21) taken pairwise.

List of the 26 gene pathways investigated

Generalities and characteristics of the volunteers ($N = 11$)
1. HALLMARK_OXIDATIVE_PHOSPHORYLATION
2. HALLMARK_FATTY_ACID_METABOLISM
3. HALLMARK_GLYCOLYSIS
4. HALLMARK_MYOGENESIS
5. HALLMARK_MTORC1_SIGNALING
6. REACTOME_GLUCOSE_METABOLISM
7. REACTOME_THE_CITRIC_ACID_TCA_CYCLE_AND_ RESPIRATORY_ELECTRON_TRANSPORT
8. REACTOME_CITRIC_ACID_CYCLE_TCA_CYCLE
9. REACTOME_FATTY_ACID_METABOLISM
10. REACTOME_GLYCOGEN_SYNTHESIS
11. REACTOME_GLYCOGEN_STORAGE_DISEASES
12. REACTOME_MITOPHAGY
13. REACTOME_MITOCHONDRIAL_FATTY_ACID_BETA_ OXIDATION
14. REACTOME_MITOCHONDRIAL_BIOGENESIS
15. REACTOME_MTORC1_MEDIATED_SIGNALLING
16. REACTOME_MUSCLE_CONTRACTION
17. BIOCARTA_MITOCHONDRIA_PATHWAY
18. BIOCARTA_AKT_PATHWAY
19. WP_OXIDATIVE_PHOSPHORYLATION
20. WP_FATTY_ACID_BETA_OXIDATION
21. WP_INSULIN_SIGNALING
22. WP_HYPERTROPHY_MODEL
23. WP_STRIATED_MUSCLE_CONTRACTION_PATHWAY
24. WP_FOCAL_ADHESION_PI3K_AKT_MTOR_SIGNALING_ PATHWAY
25. GOBP_SKELETAL_MUSCLE_ATROPHY
26. HP_SKELETAL_MUSCLE_HYPERTROPHY

Statistical analysis

A priori power analysis was performed to determine the appropriate sample size (for further details, see Sarto et al., 2022). The total sample size was 11 subjects. Therefore, the 12 participants were recruited, also considering potential study drop-outs. Normality of *in vivo* data of muscle morphology, architecture and

function, fibre CSA, and fibre type, were assessed through a Shapiro–Wilk normality test and Q–Q plots. All the considered parameters passed normality tests. For all these variables, one-way repeated-measures ANOVA (regular or mixed effects, depending on missing values) with Tukey's *post hoc* test was performed to determine whether differences among the different time points were present. For all ANOVAs, sphericity was tested with Mauchly's test and when the assumption of sphericity was violated, Greenhouse–Geisser correction was applied.

Unless stated otherwise, statistical significance was set at $P < 0.05$. GraphPad Prism (version 10.2.3; GraphPad Software, San Diego, CA, USA) was used to perform statistical analysis. Pathway scores were generated via Gene Set Variation Analysis (Hänzelmann et al., 2013) implemented in the R package GSVA v.1.48.0. Pairwise time point comparisons were performed using paired Wilcoxon tests in the base R package stats v.4.3.0.

Results

No side effects regarding biopsy procedures, ULLS exposure or the AR phase were reported.

General and anthropometric characteristics of the volunteers are reported in Table 1.

Muscle function, training-related variables and physical activity levels

MVC (Fig. 2*A*) decreased significantly over the 10 days of ULLS by −29.3% compared to baseline values (563 ± 101 *N* at LS10 *vs.* 797 ± 111 *N* at LS0, $P < 0.001$) (Sarto et al., 2022). A significant full restoration of MVC (42.9%) was observed after 21 days of AR compared to LS10 (792 ± 106 *N*, $P < 0.001$). Both 1RM values for leg press and leg extension exercises showed a significant increase at the start of each training week, and training volume kept increasing during the whole training intervention. All the variables related to the training protocol

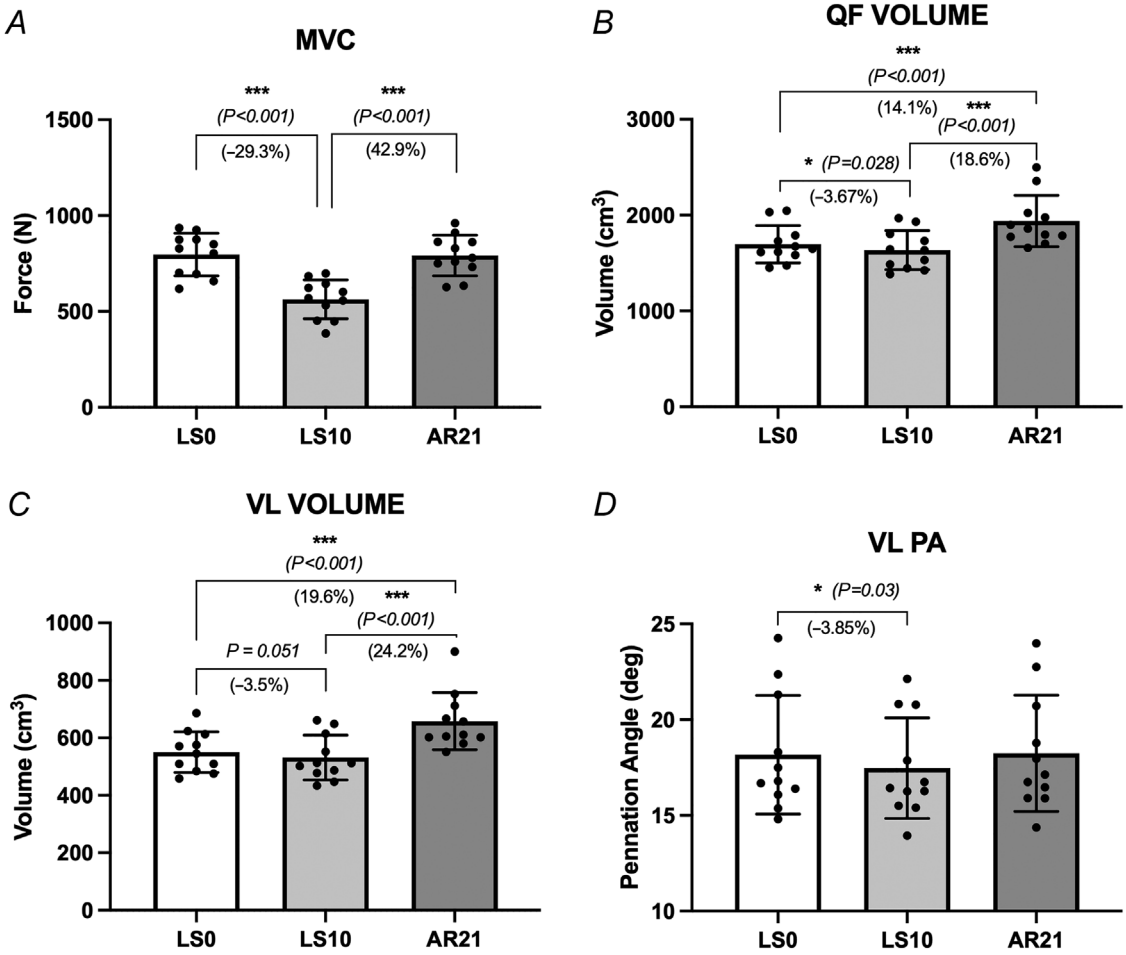

Figure 2. Adaptations in muscle function, morphology and architecture
A, maximal voluntary contraction (MVC); *B* and *C*, changes in quadriceps femoris and vastus lateralis whole muscle volume; and *D*, changes in vastus lateralis pennation angle. ***$P < 0.001$ (data are presented as mean ± SD; $N = 11$).

Table 2. Values for training load, training volume, RPE post-exercise session and muscle soreness scale for pre- and post-exercise sessions

AR21 period	Week 1	Week 2	Week 3
1RM LExt (kg)	114.1 ± 13	133.6 ± 21.1** ($P = 0.0012$)	147.2 ± 24.1***, ###
1RM LPress (kg)	55.6 ± 6.8	63.7 ± 6.3	69.7 ± 8.7
Training Vol LExt (kg)	2867.4 ± 370.8	3320.8 ± 480***	3701.4 ± 431.2***, ###
Training Vol LPress (kg)	6721.3 ± 895.2	7965.4 ± 1432.2***	8793.2 ± 1536.8***, ###
RPE post-exercise (AU)	6.3 ± 1.4	6.4 ± 2	6.1 ± 2
Soreness (pre-EX) (AU)	2.2 ± 2.1	0.9 ± 0.8	1.5 ± 1.3
Soreness (post-EX) (AU)	4.2 ± 2.1$$ ($P = 0.006$)	4.4 ± 2.4$$$	4.9 ± 2.4$$$

***$P < 0.001$ *vs.* week 1 values; ###$P < 0.001$ *vs.* week 2; $$$$P < 0.001$ compared with the pre-EX values at the same time point (data are presented as mean ± SD; $N = 11$).

employed (i.e. 1RM, training volume, rate of perceived exertion) are shown in Table 2. During the AR period, the estimated 1RM was found to be significantly increased for leg press exercise, compared to the values measured after limb suspension, by 16.8 ± 10.8% at the start of week 2 ($P = 0.0012$) and by 28.8 ± 14.6% at week 3 ($P < 0.001$), with a further significant increase by 10.3 ± 6.6 % compared to week 2 values ($P < 0.001$). In a specular manner, the estimated 1RM was found to be significantly increased also for leg extension exercise by 15.1 ± 8.9% ($P < 0.001$) and 25.4 ± 5% ($P < 0.001$) at week 2 and week 3, respectively. Similarly, a further significant change was observed between week 2 and week 3 (9.4 ± 8.2%, $P < 0.05$), confirming the intensity of exercises was progressively increased throughout the whole AR period.

The average total physical activity (MET- Metabolic Equivalent of Task- minutes per week) and sedentary time per week were calculated through the GPAQ questionnaire: total physical activity dramatically decreased (as expected) from LS0 to LS10 by −86.4% (from 3112.72 ± 1484.37 to 421.81 ± 420 MET minutes per week, $P < 0.001$) and was greater at AR21 (3809.1 ± 1775.57 MET minutes per week), also significantly greater compared with LS0 values ($P = 0.013$). Sedentary time showed, as expected, diametrically opposite trends, significantly increasing during ULLS by 45% from LS0 (4935 ± 801.62 *vs.* 3398.18 ± 1176.06 min per week, $P = 0.029$) and returning to baseline values during AR21 (3054.54 ± 1178.11 min per week).

Muscle volume, thigh lean mas and muscle architecture

Quadriceps muscle volume (Fig. 2*B*) showed a significant decrease at LS10 compared to LS0 (−3.67 ± 4%; 1634.53 ± 203.49 cm^3 *vs.* 1696.22 ± 195.03 cm^3, respectively, $P = 0.028$). VL muscle volume showed a similar trend (−3.47 ± 3.98%; 531.83 ± 78.1 cm^3 *vs.* 550.23 ± 71.02 cm^3, at LS10 and LS0, respectively, $P = 0.051$), although this was not statistically significant (Fig. 2*C*). Muscle volume for both QF and VL increased significantly at AR21 by +18.68 ± 6.87% (1938.83 ± 266.6 cm^3, $P < 0.001$) and 24.15 ± 10.4% (658.27 ± 99.73 cm^3, $P < 0.001$) respectively compared to the end of ULLS (LS10), resulting in a 14.1 ± 5.1% ($P < 0.001$) and a 19.6 ± 8% ($P < 0.001$) difference when compared to LS0.

Right thigh lean mass measured by DEXA did not show any significant change after limb suspension but increased by 2.75 ± 2.13% at AR21 compared to LS10 (9484.13 ± 959.29 g *vs.* 9230.24 ± 822.78 g, $P = 0.006$) and by 2.12 ± 2.35% compared to LS0 (9484.13 ± 959.29 g *vs.* 9287.21 ± 919.13 g, $P = 0.029$).

VL pennation angle was reduced at LS10 compared to LS0 (−3.55 ± 3.74%; 17.46 ± 2.62 degrees *vs.* 18.16 ± 3.09 degrees, $P = 0.03$, respectively). However, full restoration of PA was observed at AR21 (18.24 ± 3.04 degrees) compared to LS0 (Fig. 2*C*).

No significant changes were observed for fascicle length.

Total body water and dietary monitoring

Total body water did not change from LS0 to LS10, but it increased significantly by 3.1 ± 3.23% at AR21 compared to LS10 (42.41 ± 3.7 *vs.* 41.14 ± 3.2, $P = 0.022$, respectively) (Fig. 5*C*).

The diet diary analyses showed no significant differences either in total daily calorie intake between pre-ULLS (1946.99 ± 230.06 kcal), during ULLS (1850.99 ± 341.54 kcal) and in the AR period (1948.95 ± 429.44 kcal), or for any of the macronutrients assessed (carbohydrates, fats, proteins).

Muscle fibre CSA and phenotypical changes

Two volunteers did not agree to undergo the biopsy procedure at AR21 for personal reasons. The *N* per time point of the following analyses was $N = 11$ for LS0 and LS10 time points, and $N = 9$ for AR21. Muscle fibre CSA did not show any significant change for both type I and type II fibres after ULLS. At AR21, by contrast, type I fibre CSA was slightly, yet significantly, lower than LS0 ($-19.3 \pm 5.52\%$; 3135.81 ± 344.71 μm^2 *vs.* 3878.56 ± 216.2 μm^2, respectively; $P = 0.031$). No difference was found between LS0 and LS10. Type II CSA showed a small and not significant trend to decrease at AR21 (Fig. 3*A*, *B*).

Fibre type distribution (as detected by immunostaining) was not affected by the ULLS period but the percentage of type I fibres increased with AR by 33.96% ($P = 0.015$), while the percentage of type II fibres decreased at AR21 by −20.76% ($P = 0.015$) when compared to LS10 (Fig. 3*C*, *D*).

Myosin heavy chain content and expression of MyHC-coding genes

MyHC-IIx content obtained by SDS-PAGE and densitometry of MHC isoform bands showed just a trend to increase after ULLS compared to LS0 and to decrease at AR21 compared to LS10, but both changes did not reach statistical significance. MyHC-I also showed an opposite trend at AR21, increasing by $18.58 \pm 33.5\%$, but this change was not significant (Fig. 4*A*–*C*).

The mRNA for the gene coding for MyHC-I (i.e. MYH7) was found to be differently expressed at LS10 compared to LS0 ($-47.56 \pm 29.88\%$, $P = 0.0167$); conversely, its expression was markedly increased at AR21 compared to LS10 ($208.99 \pm 209.44\%$, $P = 0.0022$) (Fig. 4*D*). Similarly, the gene coding for MyHC-IIa (i.e. MYH2) showed a significantly suppressed expression at LS10 compared to LS0 ($-32.78 \pm 20.11\%$, $P < 0.01$), while an increased expression was observed at AR21 ($\sim 36 \pm 52\%$), although this was not statistically significant ($P = 0.082$) (Fig. 4*E*). Almost in an opposite fashion, the expression for the gene coding for MyHC-IIx (i.e. MYH1) was constant at LS10 when compared to LS0, but markedly decreased at AR21 compared to LS10 ($-85.11 \pm 20.84\%$, $P < 0.001$) and to LS0 ($-85.57 \pm 19.72\%$, $P < 0.01$) (Fig. 4*F*).

PAS and SDH staining

PAS staining was performed to investigate the behaviour of glycogen storage/content after limb suspension and AR periods (Fig. 5*A*, *B*). Glycogen content did not change after ULLS but significantly increased after AR ($+16.11 \pm 15.51\%$, $P = 0.0314$, at AR21 compared to LS10 and $+14.62 \pm 14.8\%$, $P = 0.0375$, when compared to LS0). In a similar fashion, SDH staining was not affected by ULLS but increased after training at AR21 by $20.5 \pm 9.1\%$ ($P < 0.001$) compared to LS10 and by $18.69 \pm 16.99\%$ ($P = 0.028$) compared to baseline values (Fig. 6*A*). For SDH staining, the data were evaluated only

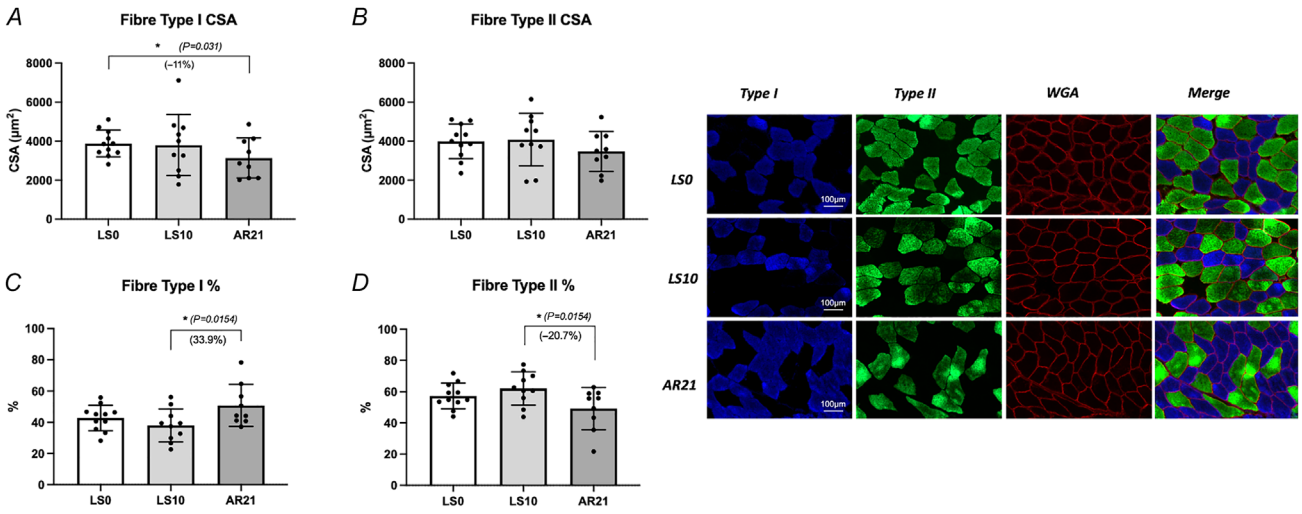

Figure 3.
A and *B*, changes in cross-sectional area (CSA) for type I (*A*) and type II (*B*) fibres; *D* and *C*, changes in fibre type I (*C*) and type II (*D*) distribution at each time point (data are presented as mean ± SD; *N* = 11 for LS0 and LS10 time points, *N* = 9 for AR21). *E*, representative muscle sections for the three different time points stained for Myosin Heavy Chain (MyHC) type I (blue), for MyHC-II (green) and for wheat germ agglutinin (WGA) (red).

on $N = 8$ volunteers across all time points due to technical issues arising from limited sample availability for one participant.

Mitochondrial protein content and signalling

As the outcomes of the SDH staining protocol pointed to an increased oxidative capacity at AR21, we decided to investigate the total level of several mitochondrial-related proteins by western blotting analyses.

PGC-1α levels showed a tendency to decrease at LS10 compared to baseline values (not significant) and then increased after AR when compared to LS10 (only marginally statistically significant, $P = 0.056$). TOM20 showed a similar non-significant trend to PGC-1α (Fig. 7).

When looking at mitochondrial pro-fusion proteins, MFN1 levels decreased at LS10 compared to LS0 but not significantly, whereas levels increased significantly at AR21 compared to LS10 ($P = 0.0147$); MFN2 levels were significantly lower at LS10 compared to baseline ($P = 0.0324$) and increased markedly at AR21 ($P = 0.0006$ *vs*. LS10). OPA1 levels increased significantly at AR21 when compared to LS10 ($P = 0.0099$) (Fig. 8).

Mitochondrial fission protein DRP1 levels tended to decrease after ULLS (although not significantly) but increased significantly at AR21 compared to LS0 ($P = 0.0185$). When looking at the amount of phosphorylated DRP1 (pDRP1) normalised to its protein level at two different phosphorylation sites (616 and 637), a very strong increase was observed at AR21 for pDRP1 616 compared to both LS10 ($P = 0.0013$) and LS0 ($P = 0.0018$), whereas a significant decrease was observed at LS10 for pDRP1 637 compared to LS0 ($P = 0.0016$) and its values failed to recover to baseline values. No significant changes were observed for FIS1 protein levels (Fig. 9).

Regarding mitochondrial complexes (CI-NDUFB8, CII-SDHB, CIII-UQCRC2, CIV-MTCO1, CV-ATP5A) no significant changes were observed throughout the whole intervention.

ULLS and active recovery transcriptomic profile

We decided to test the transcriptional reprogramming induced by RT performed after muscle unloading by targeting differentially expressed Hallmarks and Canonical Pathways that are known to be relevant to muscle physiological responses to unloading and, most importantly, to exercise, such as muscle atrophy/hypertrophy and myogenesis, as well as mitochondrial, oxidative and glucose metabolism pathways. Our analyses included specific pathways obtained from the Molecular Signatures Database (MSigDB) (Liberzon et al., 2015) (see the list in the Methods). Merging these 26 pathways, our analyses showed a significant shift in the overall oxidative and fatty acid metabolism-related transcriptomic profile (across a total of 1784 measured genes) comparing LS0 and LS10. These changes were restored at AR21, and some pathways even showed a significantly greater enrichment when

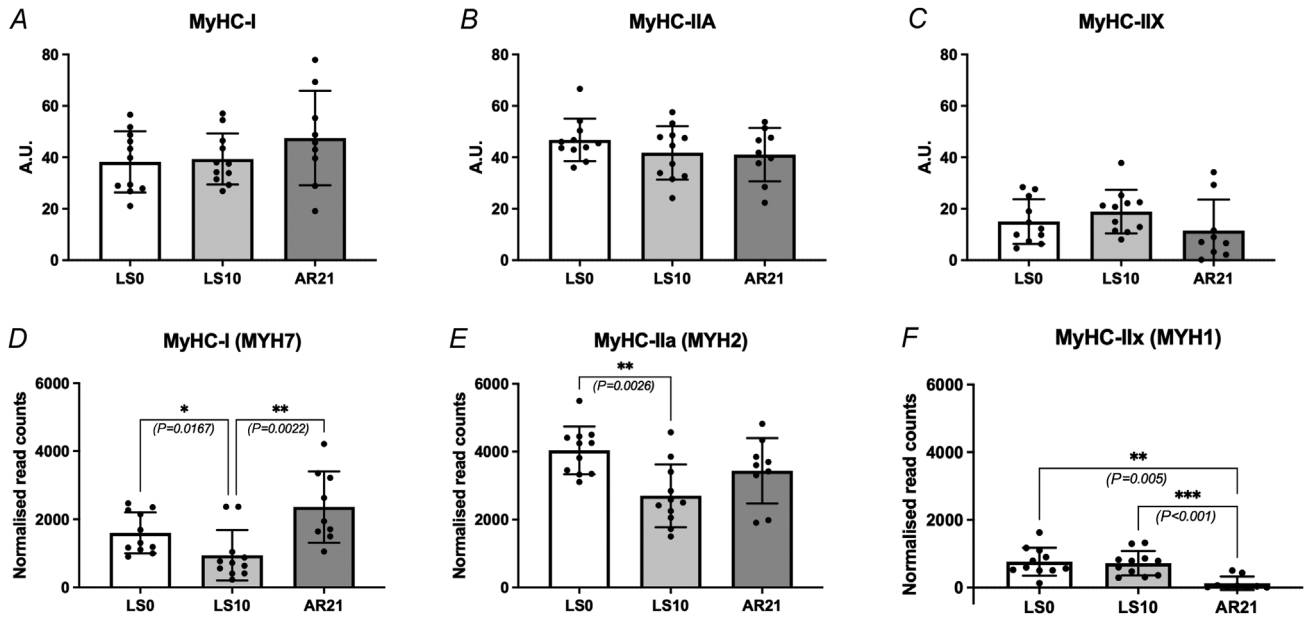

Figure 4.
A–C, Myosin Heavy Chain (MyHC) type I, IIA, and IIX content measured by SDS-PAGE; *D–F*, MHC-coding gene expression measured by RNA-seq (data are presented as mean ± SD; *N* = 11 for LS0 and LS10 time points, *N* = 9 for AR21).

compared to baseline values. The volcano plots in Fig. 10 illustrate genes compared pairwise between time points. For each volcano plot, the y-axis shows $-\log_{10}(P\text{-value})$; reference lines display the false-discovery rate (FDR) q-values 0.05 and 0.01. All the volcano plots generated were mostly symmetrical, confirming both up- and downregulation of genes related to muscle oxidative metabolism, muscle hypertrophy and muscle contraction in response to the interventions. With unloading, 882 genes were differently regulated at $q < 0.05$ (655 genes at $q < 0.01$) (Fig. 10*A*) while a total of 891 genes at $q < 0.05$ and 686 genes at $q < 0.01$ were differently expressed at AR21 (Fig. 10*B*). Some genes still showed greater enrichment at AR21 when compared to LS0: 487 genes were significantly differentially expressed at $q < 0.05$ (220 genes at $q < 0.01$) (Fig. 10*C*).

Out of the 26 pathways that were investigated, we identified, for each pairwise comparison (i.e. LS10 *vs.* LS0, AR21 *vs.* LS10, AR21 *vs.* LS0), 11 (42%) significant at $q < 0.05$ and 8 (31%) at $q < 0.01$ for LS10 *vs.* LS0, 14 (54%) pathways significant at $q < 0.05$ for AR21 *vs.* LS10, and 5 (19%) pathways significant at $q < 0.05$ for AR21 *vs.* LS0. In particular, we noted that after the AR period, compared to the end of ULLS, the top two differently enriched (i.e. positively/upregulated) gene sets were Hallmarks related to oxidative phosphorylation and fatty acid metabolism, and that pathways related to respiratory electron transport, citric acid TCA cycle and oxidative phosphorylation were amongst the most positively differently enriched ones at AR21 when compared to LS10.

We utilised the method known as Gene Set Variance Analysis (GSVA) (Hänzelmann et al., 2013) to obtain scores as measures of pathway-level expression for each sample, which subsequently allowed us to compute trajectories showing each subject's pathway scores as a function of time. Amongst those most significantly influenced by limb suspension and AR, we found oxidative phosphorylation, fatty acid metabolism, oxidative metabolism (i.e. citric acid TCA cycle and respiratory electron transport chain) and mitochondrial biogenesis, as well as pathways regulating skeletal muscle atrophy and hypertrophy (Fig. 11*A*, *B*).

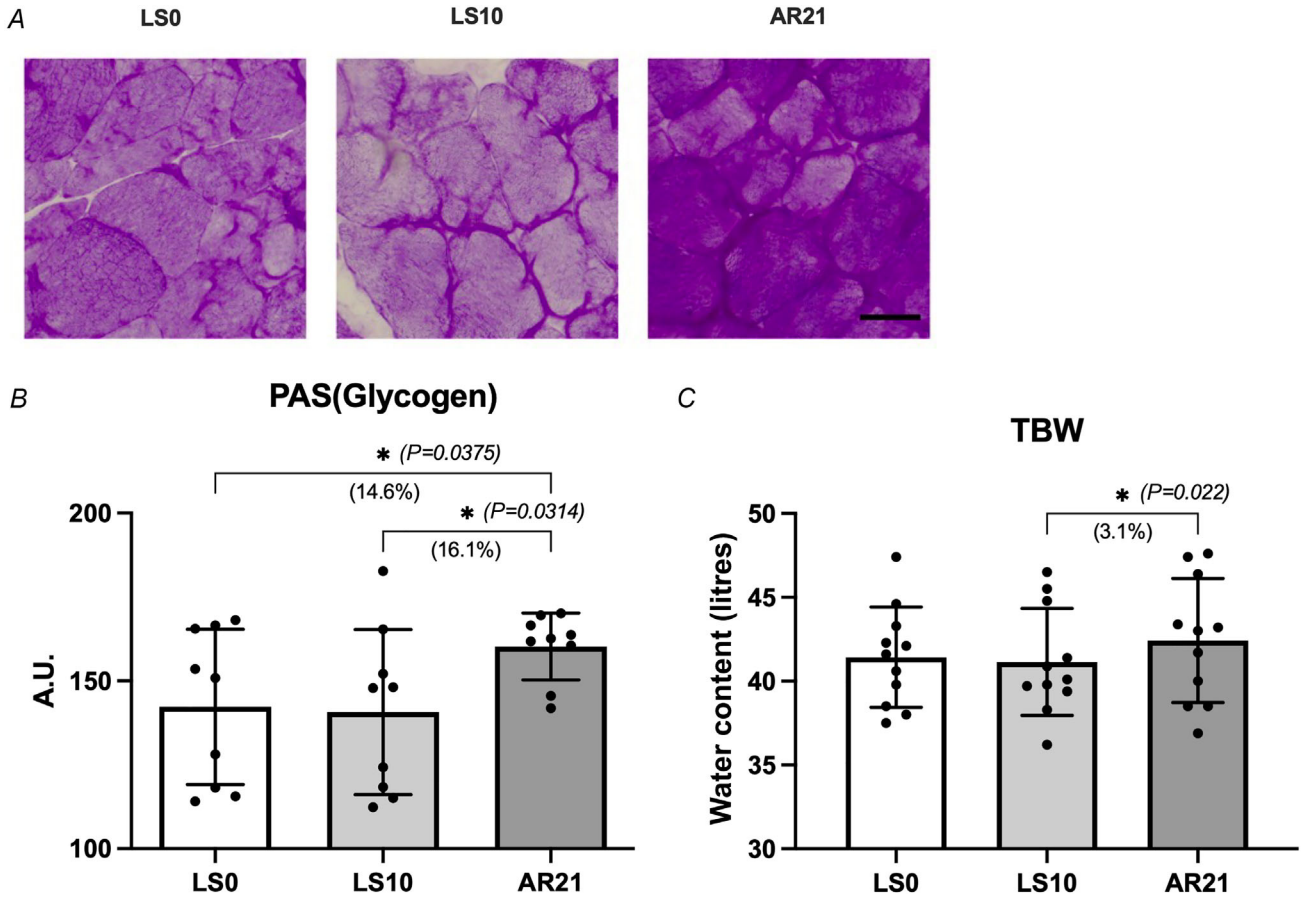

Figure 5.
A, muscle sections at the three different time points treated with periodic acid Schiff (PAS) staining protocol for muscle glycogen content analyses (scale bar = 50 µm); *B*, muscle glycogen content; *C*, total body water (TBW) measured by bioelectrical impedance analysis (BIA) (data are presented as mean ± SD; $N = 9$ for PAS, $N = 11$ for TBW).

Discussion

Ten days of ULLS led to significant decrements in whole muscle mass and strength. In line with our hypothesis, a 21 day period of AR based on RT resulted in a full recovery of muscle function, as expressed by isometric MVC values. This was accompanied by a marked increase in whole muscle volume that largely exceeded baseline values by ∼14 and 19% for QF and VL muscle, respectively. Such an unexpected increase in muscle volume after only nine sessions of resistance exercise was not matched by a corresponding increase in fibre type I or II CSA. In contrast, we identify an ∼15% increase in muscle glycogen content after the AR period, accompanied by an ∼3% increase in total body water. An ∼34% increase in type I fibre distribution with a concomitant ∼21% reduction of type II fibre was found after retraining. Surprisingly, we observed a great enhancement of gene pathways related to oxidative and fatty acid metabolism, supported by increased content and activity of proteins related to mitochondrial dynamics.

Changes in *in vivo* muscle function and whole muscle volume upon disuse and active recovery

Ten days of ULLS resulted in an ∼30% decrease in isometric MVC. Similar findings were previously reported in young males after leg casting (Suetta et al., 2009) or limb suspension (Campbell et al., 2013) (∼20% to 26% decrease in MVC, respectively). For the same participants of our study, activation capacity, central neuromodulation and motor unit properties were all affected by ULLS, confirming the neural contribution to the loss of muscle force (Martino et al., 2024; Sarto et al., 2022; Valli et al., 2023). RT was successful in restoring muscle function, as previously reported in response to 3–4 weeks of exercise (Campbell et al., 2013; Suetta et al., 2009).

In line with the literature on muscle disuse, whole quadriceps muscle volume and VL pennation angle decreased significantly by 3.7% and 3.8% at LS10, similar to previous reports (Campbell et al., 2013; de Boer et al., 2007, 2008; Kilroe et al., 2020; Suetta et al., 2009). VL muscle volume showed milder atrophy ($P = 0.051$),

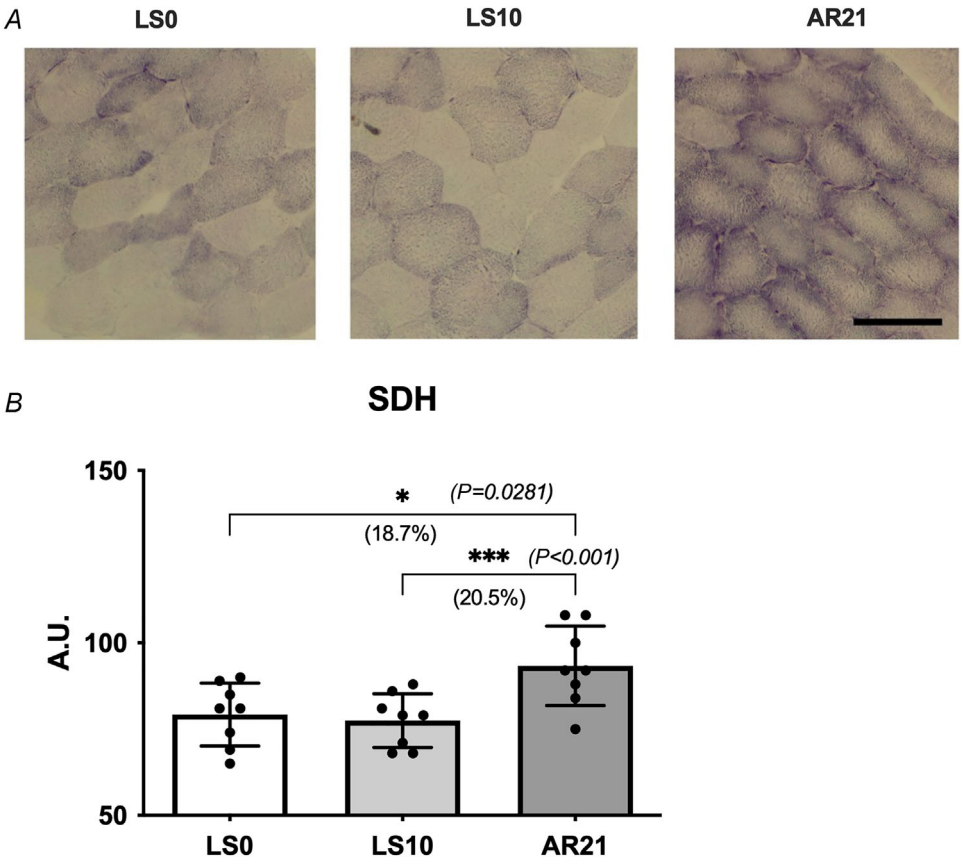

Figure 6.
A, muscle sections at the three different time points stained for succinate dehydrogenase (scale bar = 100 μm) and *B*, succinate dehydrogenase (SDH) activity (data are presented as mean ± SD; *N* = 9).

suggesting a heterogeneous response of different muscles within the same limb. The resistance exercise programme induced a change in muscle volume of unusual magnitude (∼19%). This was rather surprising considering that previous work investigating the recovery from muscle disuse with RT of similar intensity (80% 1RM), training volume and load progression used in this study showed smaller quadriceps volume increases (∼8% to 14%) (Campbell et al., 2013; Suetta et al., 2009). Moreover, even when comparing our results to the literature of muscle adaptations to strength training alone (i.e. without prior muscle disuse), the highest increase of quadriceps volume observed in humans to short-term training was 14% after 5 weeks of resistance/mixed model exercise (Lundberg et al., 2013; Tesch et al., 2017), equating to a rate of increase in muscle volume of ∼0.4% day^{-1} comparing to the ∼0.85–1% day^{-1} observed in the present study. Lastly, quadriceps muscle CSA increase has been shown to reach values around ∼20% only after 40–60 days of RT without prior disuse intervention (Wernbom et al., 2007). To assess if such an unexpected increase in volume could be attributed to hypertrophy, we investigated changes that occurred at the fibre level.

Muscle fibre CSA, fibre type distribution and MHC composition

VL type I and type II fibre CSA did not show a significant decrease after 10 days of ULLS. A loss of VL muscle volume (from which biopsies were collected) was observed but did not reach significance ($P = 0.051$). Our results are in contrast with previous reports. Suetta et al. (2012) showed an average fibre CSA decrease of ∼10% after 4 days of leg immobilisation. Similarly, fibre atrophy was found after 14 days of casting (Wall et al., 2013). Fibre atrophy was also found in other works using single-skinned muscle fibres after 35 days of bed rest (−31% type I and −21% type IIA fibres) (Brocca et al., 2012) or 3 week of ULLS (−23% type I fibres and −22% type IIA fibres) (Brocca et al., 2015; Campbell et al., 2013). The discrepancy could be due to the longer exposure time or more severe (i.e. leg casting) immobilisation used in these previous studies compared to the present one. Indeed, following bed rest, in the same subjects, muscle fibre atrophy was present after 35 days, but not after 8 days (Brocca et al., 2012). In support, Hespel et al. (2001), did not find any significant decrease in fibre type I and II CSA following 14 days of casting, whereas decrements

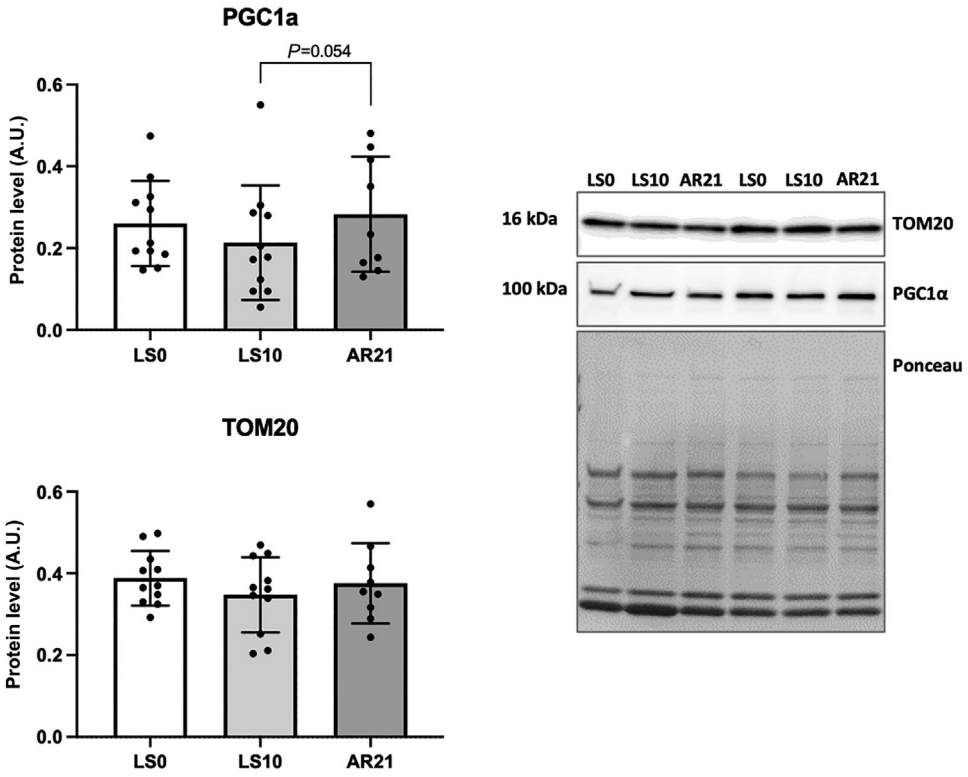

Figure 7. Quantification of protein levels by western blot analysis of PGC-1α and TOM20
Data are presented as mean ± SD; $N = 11$ for LS0 and LS10 time points, $N = 9$ for AR21.

in all fibre types were found after 21 days (Hortobágyi et al., 2000). The disuse literature suggests that fibre CSA atrophy is mostly affected by the severity and typology of the unloading model employed and the exposure time (Adams et al., 2003), occurring very rapidly (∼3/7 days) after dry immersion (the most severe model of muscle disuse on Earth) (Demangel et al., 2017; Litvinova et al., 2004), but not observed after 5–14 days of bed rest (Monti et al., 2021; Pišot et al., 2016; Reidy et al., 2018). Thus, it is plausible that atrophy of VL and its muscle fibres were simply not detectable within such a short-term disuse period.

The absence of fibre hypertrophy following the AR period, despite the increase in VL muscle volume, is surprising. Although it has been clearly established that resistance exercise alone can cause fibre hypertrophy (Aagaard et al., 2004), like our findings, a short-term RT period (∼3 weeks) performed after muscle unloading (Hespel et al., 2001) did not report significant increases of myofibre CSA. On the contrary, a longer intervention of 12 weeks of either eccentric, concentric or mixed training modalities following 3 weeks of limb immobilisation was effective in inducing both type I and II fibre hypertrophy (Hortobágyi et al., 2000). A previous project showed significant atrophy and successive hypertrophy at the fibre level after 3 weeks of ULLS and subsequent 3 week of RT (Brocca et al., 2015; Campbell et al., 2013), but data were obtained from skinned single muscle fibres, in which the measurements of fibre diameter could be unreliable due to fibre swelling.

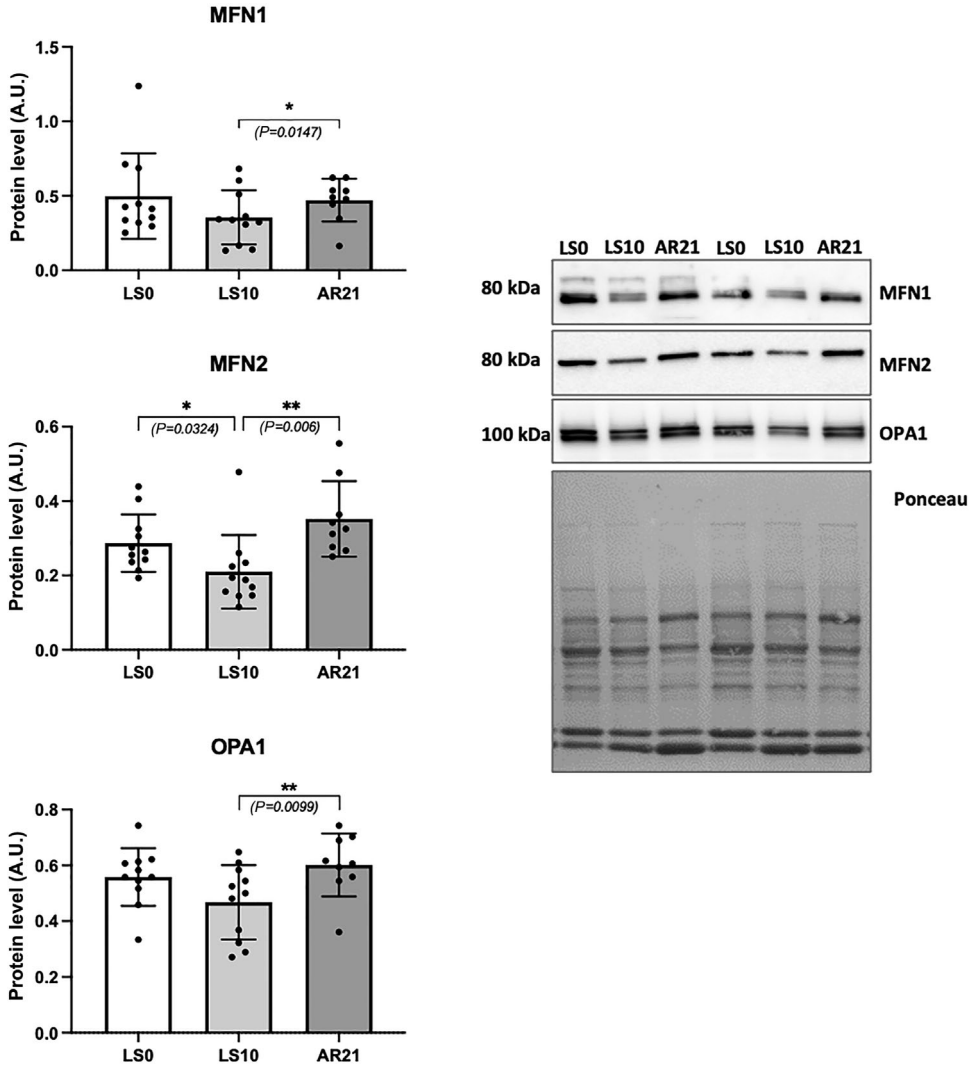

Figure 8. Quantification of mitochondrial pro-fusion protein levels by western blot analysis of MFN1, MFN2 and OPA1
Data are presented as mean ± SD; *N* = 11 for LS0 and LS10 time points, *N* = 9 for AR21.

Type I fibre distribution showed a marked increase after the AR period (∼34%), while fibre type II distribution presented almost a diametrically opposite decrease (∼−21%). This was surprising as usually type I fibres are mostly recruited to sustain forces below 20% of maximum voluntary force in isometric conditions (Gollnick et al., 1974) and the training intensity of the present study was 70% of 1RM. This would equate to an intensity in which type II fibres would be highly recruited, as already at 60% of 1RM type II fibres show a significantly greater drop in glycogen levels compared to type I (Tesch et al., 1986, 1998). In fact, the fibre type shift that we observed is usually related to endurance exercise modalities (Howald et al., 1985; Luden et al., 2012; Trappe et al., 2006). Although fibres can shift towards an MHC type II phenotype in response to long-term disuse (months rather than weeks) (Sharlo et al., 2021), this is unlikely to have completely occurred after 10 days of ULLS. In fact, the rate of turnover of myosin is 0.02–0.04% h^{-1}, that is just 1% in 24–48 h. This implies that the transition of fibre types is likely to take longer than 3 months (Holloszy & Nair, 1995). Accordingly, no significant changes were detected for MyHC isoform distribution following disuse or AR. However, the response of the single genes coding for the different MHCs (measured by RNA-seq) preceded changes in protein content as MyHC-I and MyHC-IIa expressions were significantly downregulated at LS10, whereas MyHC-IIx was not. This is in line with the slow to fast shift in MyHC isoform expression generally observed in disuse (Shenkman, 2016). RT almost completely suppressed MyHC-IIx expression, whereas it enhanced MyHC-I expression. We speculate that the increase in type I distribution can be seen as an increase in the transition of more hybrid-type fibres (potentially I/IIa).

Glycogen content and total body water

Fibre CSA did not show any increase after resistance exercise, and this could not explain the unusual magnitude of muscle volume increase. We hypothesised that part of this increase could be due to the accumulation of glycogen granules. Skeletal muscle glycogen particles are usually distributed between myofibrils and glycogen content declines in response to intense activity (Murray & Rosenbloom, 2018). The reduction of muscle glycogen during exercise is, in turn, an important regulator for glycogenesis (Zachwieja et al., 1991) and for the restoration of muscle glycogen content, which is regulated by glycogen synthase activity, insulin and blood glucose availability. In our study, muscle glycogen content was not reduced after unloading but increased significantly after the AR period (∼16% compared to LS10), presenting an over-compensatory response in glycogen storage after exercise. This was not influenced by changes in dietary habits, as the analysis of diet diaries showed that a carbohydrates consumption of ∼3 g per kg of body weight was kept constant throughout the whole study. Because

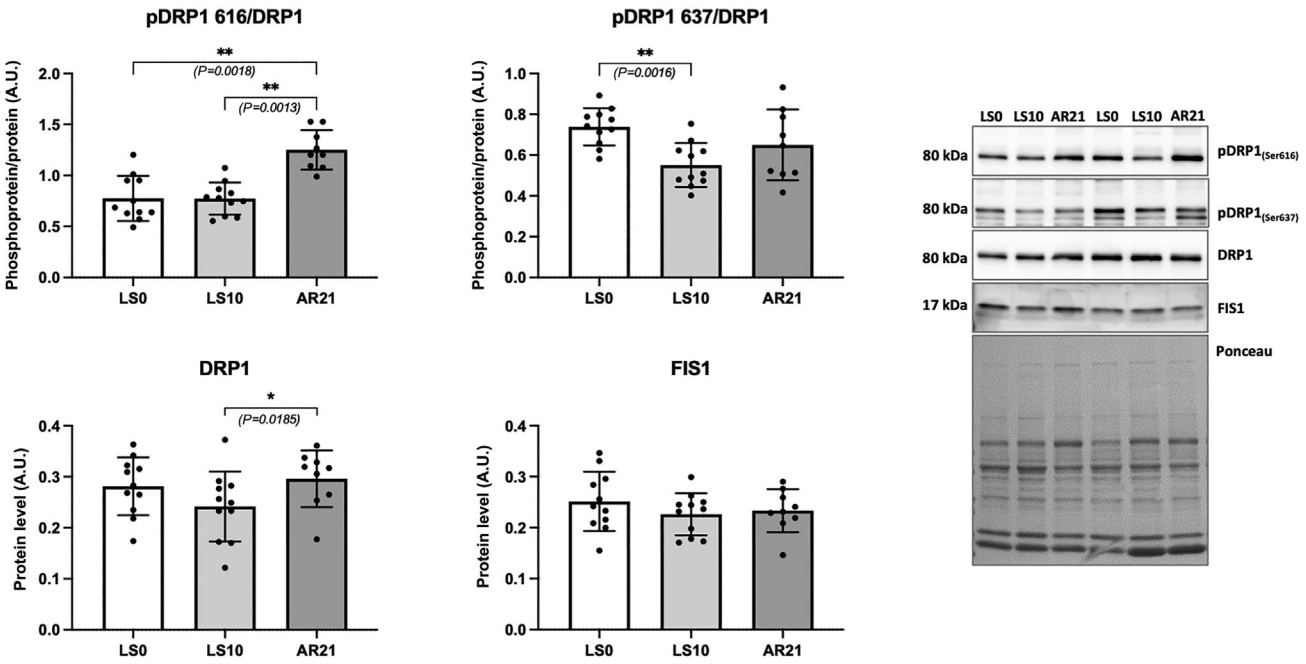

Figure 9. Determination of phosphorylation of DRP1 at two different sites (616 and 637) and quantification of mitochondrial pro-fission protein levels by western blot analysis of DRP1 and FIS1
Data are presented as mean ± SD; N = 11 for LS0 and LS10 time points, N = 9 for AR21.

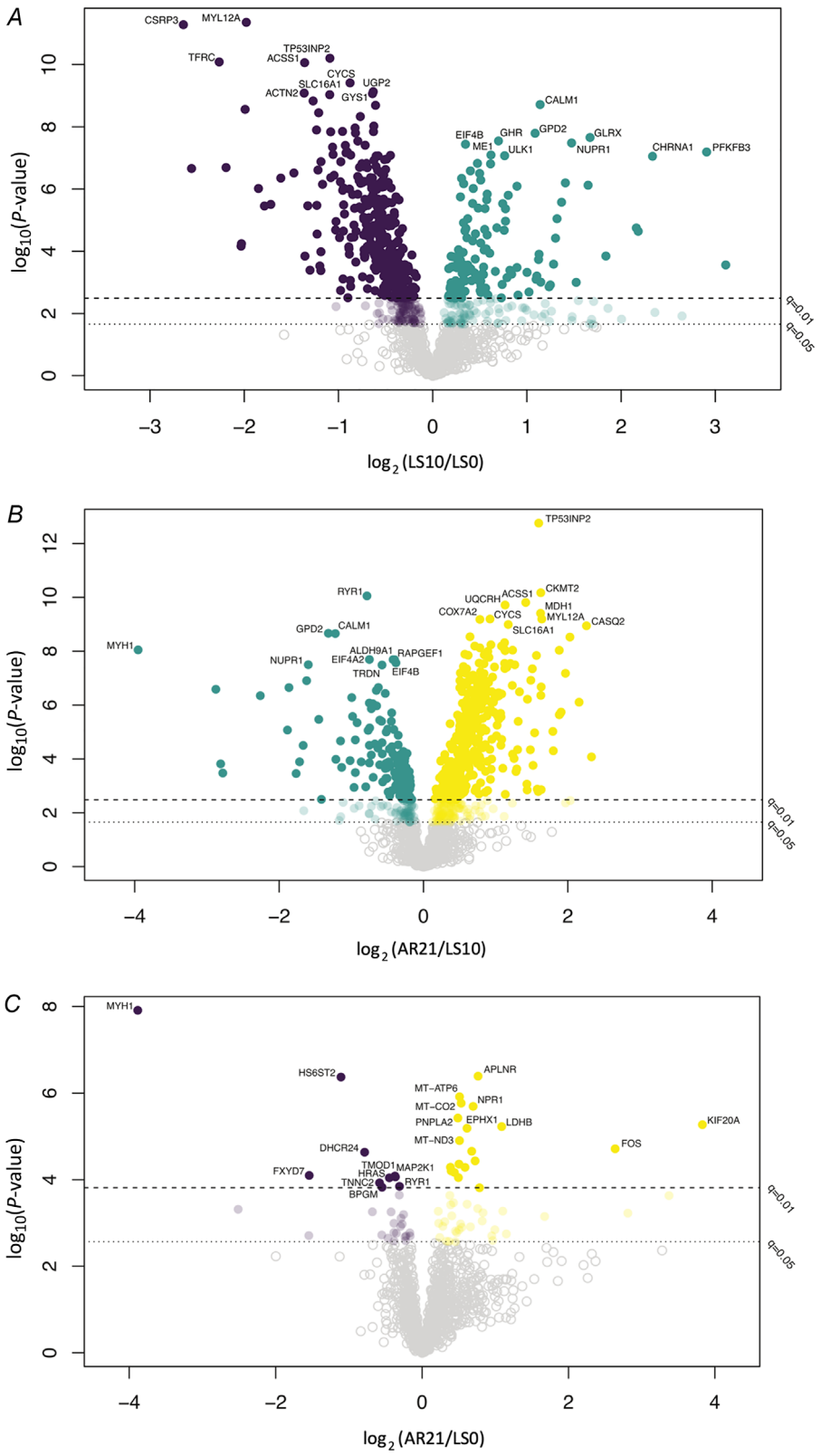

Figure 10.
A–C, volcano plots for the DEGs observed to be positively and negatively regulated at (*A*) LS10 compared to baseline (LS0), (*B*) after the active recovery period compared to LS10 and (*C*) after the active recovery period compared to LS0. *N* = 9.

each gram of glycogen is usually stored alongside 3–4 g of water (Fernández-Elías et al., 2015; Shiose et al., 2022), this could represent one of the main explanations for the marked volume increase found. In support of this, BIA identified a significant increase in total body water by ∼3% at AR21. The present data would suggest that the increase in muscle volume could have been influenced by changes in water content related to augmented glycogen storage.

Muscle glycogen has been shown to be accompanied by a preferential increase in intracellular *vs*. extracellular water (Shiose et al., 2016, 2018, 2022), and this should have been reflected by an increase in fibre size, in contrast to what was observed. However, the increase in intracellular water has been observed up to 72 h after carbohydrate loading (Shiose et al., 2016), and we could speculate that, at our time point of 21 days, a rebalancing of the intra- and extracellular water ratio might have occurred, thus obscuring potential differences in fibre CSA due to water content. An alternative possibility could be that exercising after an unloading period may have led to certain degrees of exercise-induced inflammatory response, which is known to be accompanied by oedema and expansion of extracellular water (Chazaud, 2016). In a previous study, we reported a greater expression of inflammatory gene

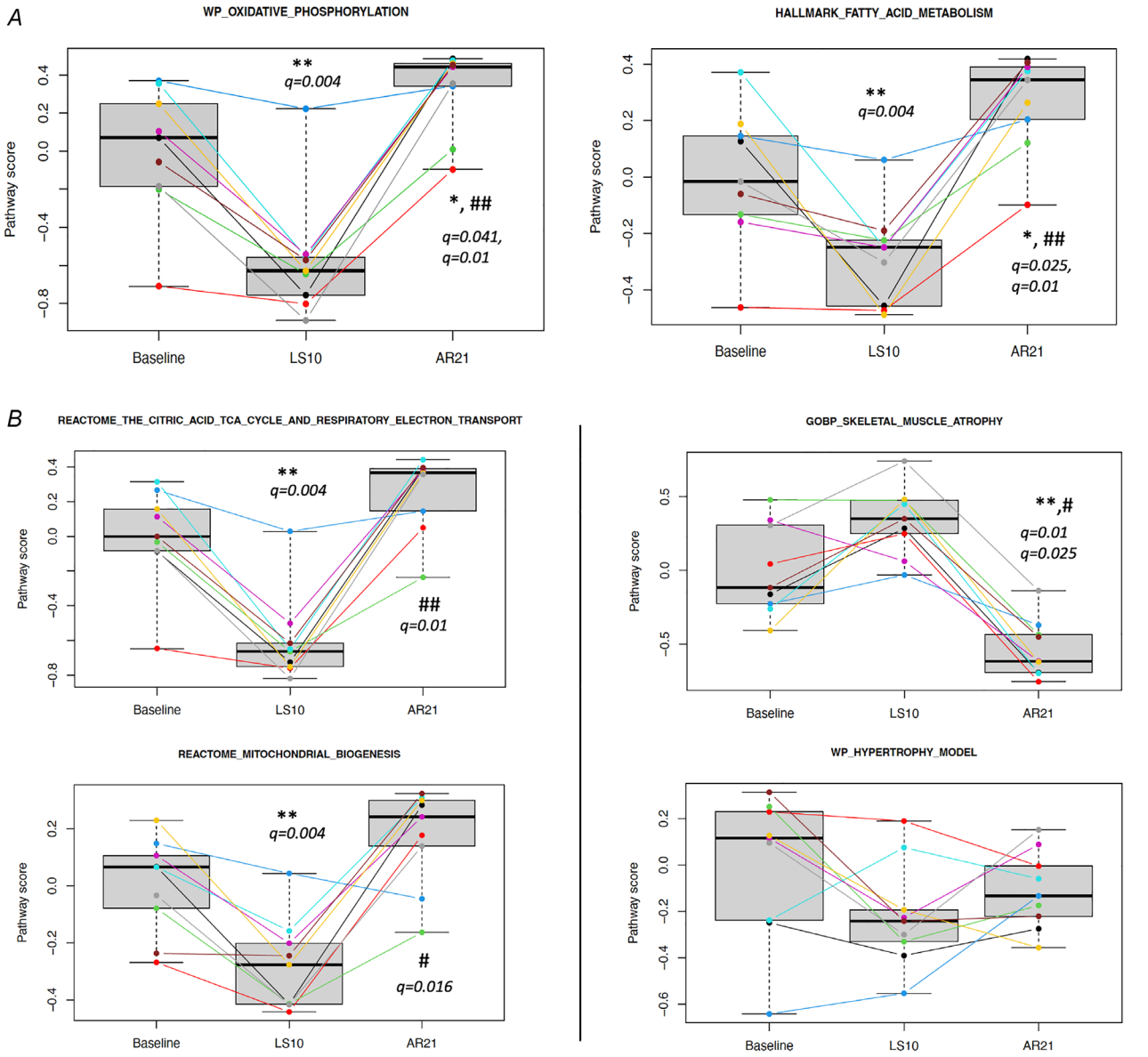

Figure 11.
A, Gene Hallmarks related to oxidative phosphorylation and fatty acid metabolism. *B*, Canonical gene pathways related to oxidative metabolism and muscle atrophy/hypertrophy. Symbols used for *q*-value significance * or ** = *vs*. LS0, # or ## = *vs*. LS10 (data in box-plots are presented as mean ± SD; *N* = 9).

pathways after ULLS (Sirago et al., 2023), and therefore it is plausible that exercise recovery may have amplified the inflammatory response that was already in place, leading to an increase in extracellular water content.

In summary, changes in whole muscle volume and pennation angle point towards a positive regulation of muscle hypertrophy after RT; however, we posit that the magnitude of whole muscle hypertrophy could have been masked by an increased water content due to a super-compensation of glycogen storage after AR and to a potential increase in exercise-derived inflammation and oedema.

Succinate dehydrogenase staining, mitochondrial protein content and signalling

Considering the augmented fibre type I distribution and glycogen content observed at AR21, we decided to investigate the modulation of markers of muscle oxidative metabolism brought by resistance exercise following short-term disuse. SDH immunoreactivity increased at AR21 above LS10 and LS0. SDH is a key mitochondrial enzyme complex (Rutter et al., 2010), and its activity has been shown to decrease by −13% after 12 weeks of RT (Chilibeck et al., 1999), while it increased in both type I and II fibres after endurance type training (12 weeks of cycling) (Chilibeck et al., 1998). Therefore, the response observed for the present study was unexpected. In a cohort of sedentary young males, skeletal muscle SDH activity increased in both type I and II fibres (but more so in type I) after 6 weeks of RT (Shepherd et al., 2014), along with enhanced muscle oxidative (i.e. COX expression) and lipid metabolism (i.e. intramuscular triglyceride utilisation). Therefore, we put forward the hypothesis by which the prior level of physical activity and a prior exposure to short-term muscle disuse could be driving the nature of adaptations to subsequent RT, suggesting that muscle could enhance metabolic recovery before hypertrophy in response to RT following disuse.

Because SDH analyses pointed towards a probably augmented muscle oxidative metabolism and mitochondrial content (Rutter et al., 2010), we investigated the total protein content and phosphorylation of key regulators of mitochondrial biogenesis, mass and mitochondrial dynamics (i.e. fusion and fission). We observed a marked regulation after ULLS and AR of a variety of mitochondrial fusion and fission proteins (MFN1, MFN2, OPA1, pDRP1 616, pDRP1 637 and DRP1) concomitantly with a trend ($P = 0.051$) for augmented mitochondrial biogenesis (∼33% increase in PGC-1α protein content at AR21 compared to LS10). Mitochondrial biogenesis promotes the abundance of high-quality mitochondria in muscle fibres and, concomitantly, a greater reduction in mitophagy is detected, until it is then no longer needed (Hood et al., 2019). Mitochondrial fusion was highly promoted by exercise, as shown by an ∼32% increase in MFN1 and an ∼73% increase in MFN2 quantity at AR21 compared to LS10, accompanied by an ∼26% increase in OPA1 content (which controls the fusion of inner mitochondrial membrane). This suggests substantial morphological remodelling of the pre-existing mitochondrial network through the increase in both outer and inner mitochondrial membrane fusion (Slavin et al., 2022), a scenario often observed in response to regular exercise. In contrast, mitochondrial fusion is often impaired during inactivity and muscle disuse, as lack of MFN2 in mice causes reductions in mitochondrial respiration together with increased reactive oxygen species (ROS) production, leading to muscle atrophy (Sebastián et al., 2016). Here, we showed a significant suppression of MFN2 (∼−30%) with only 10 days of ULLS. Conversely, the proteins regulating mitochondrial fission FIS1 and DRP1 remained unchanged at LS10 alongside pDRP1, of which phosphorylation was unchanged at the Ser616 site and, instead, significantly decreased after ULLS at the Ser637 site. The diminished activity of pDRP1637 compared to pDRP1616 may be seen as a strategy to promote fission during muscle unloading and disuse (Archer, 2013). In fact, whereas pDRP1616 regulates the translocation of DRP1 to the mitochondrial membrane, pDRP1637 reverses the process, thus inhibiting mitochondrial fission. Our data support previous observations showing that fusion is usually more diminished after disuse compared to fission (Powers et al., 2012; Sharlo et al., 2021) as DRP1 is needed to regulate fission, leading to mitophagy (Slavin et al., 2022). Interestingly, not only were mitofusins and OPA1 content (i.e. mitochondrial fusion) found to increase after RT, but also both DRP1 and pDRP1616 (i.e. mitochondrial fission) presented a significant increase at AR21, with a trend for pDRP1637 to return to baseline levels. Therefore, a fine regulation between the DRP1 phosphorylated sites promoting (616) and reversing (637) the fission process was promoted by resistance exercise, indicating an enhanced dynamic balance within fission and between mitochondrial fission and fusion.

Previous work in young healthy humans highlighted how oxidative metabolism and mitochondrial function are rapidly downregulated (within 2–3 days) in response to unloading by casting (Abadi et al., 2009), and dry immersion (Popov et al., 2023). In contrast, no change in mitochondrial content and dynamics was found after 5 days of bed rest in older males (Marshall et al., 2022), and minimal differences in mitochondrial fission were observed after 14 days of unilateral leg immobilisation in middle-aged males (Pileggi et al., 2023). The reasons behind this lack of change in mitochondrial dynamics may be related to the exposure time and the type of the disuse

intervention alongside the age of the cohorts investigated. However, the study of Pileggi et al. (2023) reported a significant reduction of MFN1 protein abundance after immobilisation and a marked increase in OPA1, MFN1 and FIS1 content after a rehabilitation programme consisting of ambulatory recovery and 2 weeks of RT, thus supporting our data.

In summary, a 21 day resistance exercise programme performed after 10 days of limb suspension was beneficial for enhancing mitochondrial activity, biogenesis and dynamics to an extent that has been only scarcely reported, mimicking more what would be expected after endurance-type exercise and not strength training per se when performed in the absence of previous muscle unloading.

Transcriptomic profile of disuse and active recovery through resistance exercise: Gene Hallmarks and pathways

To shed light on the biological mechanisms underlying muscle volume increase and enhanced mitochondrial dynamics, we performed a transcriptomic analysis to examine transcriptional changes induced by RT performed after muscle unloading. We targeted differentially expressed Hallmarks/Gene Pathways related to physiological responses to exercise, such as muscle hypertrophy, myogenesis, mitochondrial, oxidative and glucose metabolism pathways (refer to the Methods section for a more detailed description). Hallmarks and Canonical Gene Pathways related to oxidative phosphorylation and fatty acid metabolism (Fig. 11*A*) showed a dramatic downregulation at LS10, but also a complete restoration, or even an increased expression already after 21 days of AR when compared to LS0. Instead, hallmarks and pathways related to the regulation of muscle hypertrophy and mTORC1 signalling were not significantly changed after ULLS or AR; only the HALLMARK_MYOGENESIS and WP_STRIATED_MUSCLE_CONTRACTION_PATHWAY were found to be significantly enhanced at AR21 ($q = 0.012$ and $q = 0.008$, respectively). These hallmarks and pathways not only showed smaller GSVA scores compared to those related to oxidative and fatty acid metabolism, but some of the latter also showed an increased expression after AR when compared to LS0 (see Supporting Information). The pathway of mTORC1 signalling did not show any significant change as mTOR pathway expression is not always connected to hypertrophy (Phillips et al., 2013), and this was similar to the pathway related to the hypertrophy model. In addition, GOBP_SKELETAL_MUSCLE_ATROPHY pathway expression showed a trend of being positively modulated by disuse and, conversely, a significant suppression at AR21. In support of these observations, the myostatin gene (i.e. an inhibitor of muscle growth; Carnac et al., 2006) was found to be highly expressed at LS10 and to return to baseline values after AR, suggesting that muscle hypertrophy was not suppressed. PGC-1α gene expression, instead, confirmed the promotion of mitochondrial biogenesis and oxidative function (Fig. 12).

The present data find support in earlier (Abadi et al., 2009; Powers et al., 2012; Timmons et al., 2006) and recent (Miotto et al., 2019; Stokes et al., 2020) reports showing that alterations in mitochondrial transcripts are a signature of muscle disuse. However, the present study is the first to show mostly metabolic and mitochondrial transcriptional adaptations to short-term RT in the same volunteers who previously underwent 10 days of ULLS. Stokes et al. (2020), employing a within-subject study design, observed abundant regulation of mitochondrial and angiogenic gene networks and of myofibrillar protein synthesis after RT. The authors speculated that mitochondria supported angiogenesis (Diebold et al., 2019) which may have helped in enhancing muscle hypertrophy.

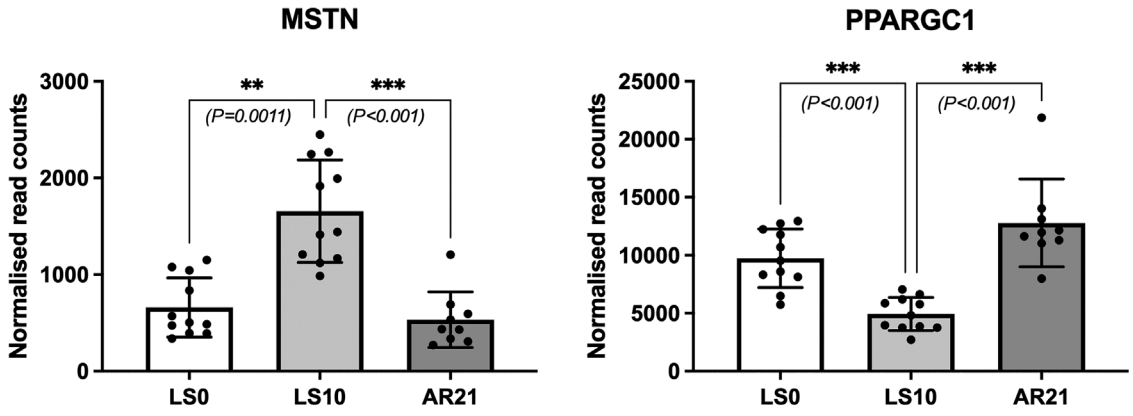

Figure 12. Expression of the genes coding for myostatin (MSTN) and PGC1-alpha (PPARGC1) proteins
Data are presented as mean ± SD; $N = 11$ for LS0 and LS10 time points, $N = 9$ for AR21.

Pillon et al. (2020) exploited 66 published data sets on human muscle transcriptomic responses to inactivity and exercise showing that inactivity was associated with reduction in mitochondrial processes (as in our study) but that only aerobic exercise (and not resistance exercises) promoted metabolic pathways and mitochondrial function, leading to an increase in the expression of genes coding for lipid-regulating enzymes and mitochondrial complexes (Pillon et al., 2020). It must be emphasised that the responses described by Pillon et al. (2020) are specific to either inactivity and unloading paradigms or exercise protocols carried out independently of each other; instead, in our study, we show the specific responses of muscles from the same subjects undergoing unloading and successive re-loading.

Thus, here we showed that a period of short-term disuse may dictate the nature of the muscle adaptations to subsequent resistance exercise, which mostly aim to restore metabolic function of skeletal muscle, promoting glucose and lipid metabolism, and, importantly, mitochondrial biogenesis and oxidative function. Although we did not measure muscle protein synthetic response in our study, we speculate that the promotion of mitochondrial pathways through resistance exercise could be seen as a potential inner muscle programme activated in response to short-term disuse irrespective of the exercise modality, where simple mechanical loading is needed to primarily restore metabolic alterations induced by unloading.

Transcriptomic profile of disuse and active recovery: top differentially expressed genes

The main transcriptomics muscle response after a short period of disuse was focused on reduced mitochondrial dynamics (TFRC, CYCS), glycogen synthesis (GYS1 and UGP2), and contraction and myogenesis (MYL12A, ACTN2 mainly involved in contraction and CSRP3 mainly involved in myogenesis) (Fig. 10*A*).

A subsequent period of retraining reduced the expression of genes such as RYR1, CALM1 and GPD2, mainly involved in Ca^{2+} handling even at the mitochondrial level, suggesting restored Ca^{2+} handling after a period of disuse and favoured by exercise. In accordance with our histological results, MYH1, the gene coding for myosin heavy chain type IIx, was significantly suppressed after AR (Fig. 10*B*). Conversely, the top regulated genes after RT showed a marked involvement of mitochondrial-related genes (CKMT2, UQCRH, ACSS1, MDH1, COX7A2, CYCS and SLC16A1) and of CASQ2 gene coding for calsequestrin 2, a protein that has been shown to be usually downregulated after bed rest (Monti et al., 2021) and that is a typical isoform of type I fibres (Murgia et al., 2021), reinforcing our conceptual idea that, here, resistance exercised had an influence on slow fibre type rather than what is usually observed.

Among the genes that showed a positive 'rebound effect' after exercise compared to baseline values, genes related to mitochondrial function (such as MT-ATP6, MT-CO2 and MT-ND3) and lipid metabolism (PNPLA2, NPR1 and EPHX1) were markedly expressed (Fig. 10*C*). The top upregulated gene was APLNR, coding for apelin receptor protein, which was also observed by Stokes et al. (2020). Essentially, the Apelin receptor is observed to play a role in sarcopenia and ageing positively regulating inter-myofibrillar mitochondrial content (Vinel et al., 2018): we speculate that ULLS, in this case, could have represented a sort of 'accelerated muscle ageing' and as APLNR is extremely well-expressed after re-loading, it may not only act as a muscle sarcopenia gene.

In summary, muscle unloading led to a marked downregulation of hallmarks and pathways mostly responsible for oxidative and fatty acid metabolism with reduced expression of genes related to mitochondrial dynamics, glycogen synthesis, myogenesis and cellular integrity. Three weeks of RT promoted a marked recovery and upregulation of hallmarks and pathways regulating oxidative metabolism, with enhanced expression of genes controlling mitochondrial function and stress, lipid metabolism and calcium handling.

Conclusions

An AR period based on RT was successful in recovering functional and structural muscle properties after 10 days of disuse, but in contrast with what is usually observed in response to strength training, oxidative metabolism and slow fibre type were mostly affected by disuse and recovery, suggesting that muscle could enhance metabolic recovery before hypertrophy in response to resistance exercise following muscle disuse. These novel observations deriving from the transcriptomic analyses point towards a marked reprogramming of skeletal muscle oxidative metabolism after AR following short-term disuse. As inactivity and muscle disuse are frequent phenomena associated with sedentary lifestyles or with limb or whole-body immobilisation due to illness and hospitalisation, the present study points to meaningful translational applications, especially for clinical and rehabilitation settings.

References

Aagaard, P., Andersen, J. L., Dyhre-Poulsen, P., Leffers, A.-M., Wagner, A., Magnusson, S. P., Halkjær-Kristensen, J., & Simonsen, E. B. (2004). A mechanism for increased contractile strength of human pennate muscle in response to strength training: Changes in muscle architecture. *The Journal of Physiology*, **534**(2), 613–623.

Abadi, A., Glover, E. I., Isfort, R. J., Raha, S., Safdar, A., Yasuda, N., Kaczor, J. J., Melov, S., Hubbard, A., Qu, X., Phillips, S. M., & Tarnopolsky, M. (2009). Limb immobilization induces a coordinate down-regulation of mitochondrial and other metabolic pathways in men and women. *PLoS ONE*, **4**(8), e6518.

Adams, G. R., Caiozzo, V. J., & Baldwin, K. M. (2003). Skeletal muscle unweighting: Spaceflight and ground-based models. *Journal of Applied Physiology (1985)*, **95**(6), 2185–2201.

Alibegovic, A. C., Sonne, M. P., Højbjerre, L., Bork-Jensen, J., Jacobsen, S., Nilsson, E., Færch, K., Hiscock, N., Mortensen, B., Friedrichsen, M., Stallknecht, B., Dela, F., & Vaag, A. (2010). Insulin resistance induced by physical inactivity is associated with multiple transcriptional changes in skeletal muscle in young men. *American Journal of Physiology-Endocrinology and Metabolism*, **299**(5), E752–E763.

Archer, S. L. (2013). Mitochondrial dynamics–mitochondrial fission and fusion in human diseases. *New England Journal of Medicine*, **369**(23), 2236–2251.

Atherton, P. J., Greenhaff, P. L., Phillips, S. M., Bodine, S. C., Adams, C. M., & Lang, C. H. (2016). Control of skeletal muscle atrophy in response to disuse: Clinical/preclinical contentions and fallacies of evidence. *American Journal of Physiology-Endocrinology and Metabolism*, **311**(3), E594–E604.

Aubertin-Leheudre, M., Pion, C. H., Vallée, J., Marchand, S., Morais, J. A., Bélanger, M., & Robitaille, R. (2020). Improved human muscle biopsy method to study neuromuscular junction structure and functions with aging. *Journals of Gerontology-Series A, Biological Sciences and Medical Sciences*, **75**(11), 2098–2102.

Beachle, T. R., & Earle, R. (1994). *Essentials of strength training and conditioning*. NSCA, Human Kinetics.

Berg, H. E., Dudley, G. A., Haggmark, T., Ohlsen, H., & Tesch, P. A. (1991). Effects of lower limb unloading on skeletal muscle mass and function in humans. *Journal of Applied Physiology*, **70**(4), 1882–1885.

Bleeker, M. W. P., Hopman, M. T. E., Rongen, G. A., & Smits, P. (2004). Unilateral lower limb suspension can cause deep venous thrombosis. *American Journal of Physiology-Regulatory, Integrative and Comparative Physiology*, **286**(6), R1176–R1177.

de Boer, M. D., Maganaris, C. N., Seynnes, O. R., Rennie, M. J., & Narici, M. V. (2007). Time course of muscular, neural and tendinous adaptations to 23 day unilateral lower-limb suspension in young men. *The Journal of Physiology*, **583**(3), 1079–1091.

de Boer, M. D., Seynnes, O. R., di Prampero, P. E., Pišot, R., Mekjavić, I. B., Biolo, G., & Narici, M. V. (2008). Effect of 5 weeks horizontal bed rest on human muscle thickness and architecture of weight bearing and non-weight bearing muscles. *European Journal of Applied Physiology*, **104**(2), 401–407.

Booth, F. W., Roberts, C. K., Thyfault, J. P., Ruegsegger, G. N., & Toedebusch, R. G. (2017). Role of inactivity in chronic diseases: Evolutionary insight and pathophysiological mechanisms. *Physiological Reviews*, **97**(4), 1351–1402.

Brocca, L., Cannavino, J., Coletto, L., Biolo, G., Sandri, M., Bottinelli, R., & Pellegrino, M. A. (2012). The time course of the adaptations of human muscle proteome to bed rest and the underlying mechanisms. *The Journal of Physiology*, **590**(20), 5211.

Brocca, L., Longa, E., Cannavino, J., Seynnes, O., de Vito, G., Mcphee, J., Narici, M., Pellegrino, M. A., & Bottinelli, R. (2015). Human skeletal muscle fibre contractile properties and proteomic profile: Adaptations to 3 weeks of unilateral lower limb suspension and active recovery. *The Journal of Physiology*, **593**(24), 5361.

Brzycki, M. (1993). Strength testing—predicting a one-rep max from reps-to-fatigue. *Journal of Physical Education, Recreation & Dance*, **64**(1), 88–90.

Campbell, E. L., Seynnes, O. R., Bottinelli, R., Mcphee, J. S., Atherton, P. J., Jones, D. A., Butler-Browne, G., & Narici, M. V. (2013). Skeletal muscle adaptations to physical inactivity and subsequent retraining in young men. *Biogerontology*, **14**(3), 247–259.

Carnac, G., Ricaud, S., Vernus, B., & Bonnieu, A. (2006). Myostatin: Biology and clinical relevance. *Mini – Reviews in Medicinal Chemistry*, **6**(7), 765–770.

Chazaud, B. (2016). Inflammation during skeletal muscle regeneration and tissue remodeling: Application to exercise-induced muscle damage management. *Immunology and Cell Biology*, **94**(2), 140–145.

Chilibeck, P. D., Bell, G. J., Socha, T., & Martin, T. (1998). The effect of aerobic exercise training on the distribution of succinate dehydrogenase activity throughout muscle fibres. *Canadian Journal of Applied Physiology*, **23**(1), 74–86.

Chilibeck, P. D., Syrotuik, D. G., & Bell, G. J. (1999). The effect of strength training on estimates of mitochondrial density and distribution throughout muscle fibres. *European Journal of Applied Physiology and Occupational Physiology*, **80**(6), 604–609.

Cook, D. B., O'connor, P. J., Eubanks, S. A., Smith, J. C., & Lee, M. (1997). Naturally occurring muscle pain during exercise: Assessment and experimental evidence. *Medicine and Science in Sports and Exercise*, **29**(8), 999–1012.

Daley, T., & Smith, A. D. (2013). Predicting the molecular complexity of sequencing libraries. *Nature Methods*, **10**(4), 325.

Demangel, R., Treffel, L., Py, G., Brioche, T., Pagano, A. F., Bareille, M. P., Beck, A., Pessemesse, L., Candau, R., Gharib, C., Chopard, A., & Millet, C. (2017). Early structural and functional signature of 3-day human skeletal muscle disuse using the dry immersion model. *The Journal of Physiology*, **595**(13), 4301–4315.

Diebold, L. P., Gil, H. J., Gao, P., Martinez, C. A., Weinberg, S. E., & Chandel, N. S. (2019). Mitochondrial complex III is necessary for endothelial cell proliferation during angiogenesis. *Nature Metabolism*, **1**(1), 158–171.

Dietrichson, P., Coakley, J., Smith, P. E., Griffiths, R. D., Helliwell, T. R., & Edwards, R. H. (1987). Conchotome and needle percutaneous biopsy of skeletal muscle. *Journal of Neurology, Neurosurgery, and Psychiatry*, **50**(11), 1461–1467.

Dirks, M. L., Miotto, P. M., Goossens, G. H., Senden, J. M., Petrick, H. L., van Kranenburg, J., van Loon, L. J. C., & Holloway, G. P. (2020). Short-term bed rest-induced insulin resistance cannot be explained by increased mitochondrial H2 O2 emission. *The Journal of Physiology*, **598**(1), 123–137.

Dobin, A., Davis, C. A., Schlesinger, F., Drenkow, J., Zaleski, C., Jha, S., Batut, P., Chaisson, M., & Gingeras, T. R. (2013). STAR: Ultrafast universal RNA-seq aligner. *Bioinformatics*, **29**(1), 15–21.

Dulac, M., Hajj-Boutros, G., Sonjak, V., Faust, A., Hussain, S. N. A., Chevalier, S., Dionne, I. J., Morais, J. A., & Gouspillou, G. (2025). A multimodal exercise countermeasure prevents the negative impact of head-down tilt bed rest on muscle volume and mitochondrial health in older adults. *The Journal of Physiology*, **603**(13), 3813–3836.

Elam, C., Hvid, L. G., Christensen, U., Kjær, M., Peter Magnusson, S., Aagaard, P., Käll, L. B., & Suetta, C. (2022). Effects of age on muscle power, postural control and functional capacity after short-term immobilization and retraining. *Journal of Musculoskeletal & Neuronal Interactions*, **22**, 486.

Fernandez, X., Lefaucheur, L., & Čandek, M. (1995). Comparative study of two classifications of muscle fibres: Consequences for the photometric determination of glycogen according to fibre type in red and white muscle of the pig. *Meat Science*, **41**(2), 225–235.

Fernández-Elías, V. E., Ortega, J. F., Nelson, R. K., & Mora-Rodriguez, R. (2015). Relationship between muscle water and glycogen recovery after prolonged exercise in the heat in humans. *European Journal of Applied Physiology*, **115**(9), 1919–1926.

Folland, J. P., & Williams, A. G. (2007). The adaptations to strength training: Morphological and neurological contributions to increased strength. *Sports Medicine (Auckland, N.Z.)*, **37**(2), 145–168.

Foster, C., Hector, L., Welsh, R., Schrager, M., Green, M., & Snyder, A. (1995). Effects of specific versus cross-training on running performance. *European Journal of Applied Physiology and Occupational Physiology*, **70**(4), 367–372.

Franchi, M. V., Atherton, P. J., Reeves, N. D., Flück, M., Williams, J., Mitchell, W. K., Selby, A., Beltran Valls, R. M., & Narici, M. V. (2014). Architectural, functional and molecular responses to concentric and eccentric loading in human skeletal muscle. *Acta Physiologica*, **210**(3), 642–654.

Franchi, M. V., Badiali, F., Sarto, F., Müller, P., Müller, N. G., Rehfeld, K., Monti, E., Rankin, D., Longo, S., Lund, J., Hökelmann, A., & Narici, M. (2022). Neuromuscular aging: A case for the neuroprotective effects of dancing. *Gerontology*, **69**(1), 1–9.

Franchi, M. V., Monti, E., Carter, A., Quinlan, J. I., Herrod, P. J. J., Reeves, N. D., & Narici, M. V. (2019). Bouncing back! Counteracting muscle aging with plyometric muscle loading. *Frontiers in Physiology*, **10**, 178.

Franchi, M. V., Ruoss, S., Valdivieso, P., Mitchell, K. W., Smith, K., Atherton, P. J., Narici, M. V., & Flück, M. (2018). Regional regulation of focal adhesion kinase after concentric and eccentric loading is related to remodelling of human skeletal muscle. *Acta Physiologica*, **223**(3), e13056.

Franchi, M. V., Sarto, F., Simunič, B., Pišot, R., & Narici, M. V. (2022). Early changes of hamstrings morphology and contractile properties during 10 days of complete inactivity. *Medicine and Science in Sports and Exercise*, **54**(8), 1346–1354.

Franchi, M. V., Wilkinson, D. J., Quinlan, J. I., Mitchell, W. K., Lund, J. N., Williams, J. P., Reeves, N. D., Smith, K., Atherton, P. J., & Narici, M. V. (2015). Early structural remodeling and deuterium oxide-derived protein metabolic responses to eccentric and concentric loading in human skeletal muscle. *Physiological Reports*, **3**(11), e12593–e12593.

Giacomello, E., Crea, E., Torelli, L., Bergamo, A., Reggiani, C., Sava, G., & Toniolo, L. (2020). Age dependent modification of the metabolic profile of the tibialis anterior muscle fibers in C57BL/6J mice. *International Journal of Molecular Sciences*, **21**(11), 3923.

Gollnick, P. D., Karlsson, J., Piehl, K., & Saltin, B. (1974). Selective glycogen depletion in skeletal muscle fibres of man following sustained contractions. *The Journal of Physiology*, **241**(1), 59–67.

Hänzelmann, S., Castelo, R., & Guinney, J.(2013). GSVA: Gene set variation analysis for microarray and RNA-seq data. *Biomedical Central Bioinformatics [Electronic Resource]*, **14**(1), 7.

Harrow, J., Frankish, A., Gonzalez, J. M., Tapanari, E., Diekhans, M., Kokocinski, F., Aken, B. L., Barrell, D., Zadissa, A., Searle, S., Barnes, I., Bignell, A., Boychenko, V., Hunt, T., Kay, M., Mukherjee, G., Rajan, J., Despacio-Reyes, G., Saunders, G., … Hubbard, T. J. (2012). GENCODE: The reference human genome annotation for The ENCODE Project. *Genome Research*, **22**(9), 1760.

Hespel, P., Op't Eijnde, B., Leemputte, M. V., Ursø, B., Greenhaff, P. L., Labarque, V., Dymarkowski, S., Hecke, P. V., & Richter, E. A. (2001). Oral creatine supplementation facilitates the rehabilitation of disuse atrophy and alters the expression of muscle myogenic factors in humans. *The Journal of Physiology*, **536**(2), 625–633.

Holloszy, J. O., & Nair, K. S. (1995). Muscle protein turnover: Methodological issues and the effect of aging. *The Journals of Gerontology: Series A*, **50A**, 107–112.

Hood, D. A., Memme, J. M., Oliveira, A. N., & Triolo, M. (2019). Maintenance of skeletal muscle mitochondria in health, exercise, and aging. *Annual Review of Physiology*, **81**(1), 19–41.

Hortobágyi, T., Dempsey, L., Fraser, D., Zheng, D., Hamilton, G., Lambert, J., & Dohm, L. (2000). Changes in muscle strength, muscle fibre size and myofibrillar gene expression after immobilization and retraining in humans. *The Journal of Physiology*, **524**(1), 293–304.

Howald, H., Hoppeler, H., Claassen, H., Mathieu, O., & Straub, R. (1985). Influences of endurance training on the ultrastructural composition of the different muscle fiber types in humans. *Pflugers Archiv: European journal of physiology*, **403**(4), 369–376.

Kang, D., Gho, Y. S., Suh, M., & Kang, C. (2002). Highly sensitive and fast protein detection with Coomassie brilliant blue in sodium dodecyl sulfate-polyacrylamide gel electrophoresis [5]. *Bulletin of the Korean Chemical Society*, **23**, 1511–1512.

Kilroe, S. P., Fulford, J., Jackman, S. R., Van Loon, L. J. C., & Wall, B. T. (2020). Temporal muscle-specific disuse atrophy during one week of leg immobilization. *Medicine and Science in Sports and Exercise*, **52**(4), 944–954.

Komi, P. V., Medical Commission, I. O. C., & Medicine, I. F. S. (2003). *Strength and power in sport*. Blackwell Science.

Kubo, K., Akima, H., Ushiyama, J., Tabata, I., Fukuoka, H., Kanehisa, H., & Fukunaga, T. (2004). Effects of 20 days of bed rest on the viscoelastic properties of tendon structures in lower limb muscles. *British Journal of Sports Medicine*, **38**(3), 324–330.

Laemmli, U. K. (1970). Cleavage of structural proteins during the assembly of the head of bacteriophage T4. *Nature*, **227**(5259), 680–685.

Law, C. W., Chen, Y., Shi, W., & Smyth, G. K. (2014). Voom: Precision weights unlock linear model analysis tools for RNA-seq read counts. *Genome Biology*, **15**(2), 1–17.

Li, B., & Dewey, C. N. (2011). RSEM: Accurate transcript quantification from RNA-Seq data with or without a reference genome. *Biomedical Central Bioinformatics [Electronic Resource]*, **12**(1), 1–16.

Liberzon, A., Birger, C., Thorvaldsdóttir, H., Ghandi, M., Mesirov, J. P., & Tamayo, P. (2015). The Molecular Signatures Database (MSigDB) hallmark gene set collection. *Cell Systems*, **1**(6), 417–425.

Litvinova, K. S., Vikhlyantsev, I. M., Kozlovskaya, I. B., Podlubnaya, Z. A., & Shenkman, B. S. (2004). Effects of artificial support stimulation on fiber and molecular characteristics of soleus muscle in men exposed to 7-day dry immersion. *Journal of Gravitational Physiology*, **11**, P131–P132.

Lowry, O. H., Rosebrough, N. J., Farr, A. L., & Randall, R. J. (1951). Protein measurement with the Folin phenol reagent. *Journal of Biological Chemistry*, **193**(1), 265–275.

Lucas, C. A., Kang, L. H. D., & Hoh, J. F. Y. (2000). Mono-specific antibodies against the three mammalian fast limb Myosin Heavy Chains. *Biochemical and Biophysical Research Communications*, **272**(1), 303–308.

Luden, N., Hayes, E., Minchev, K., Louis, E., Raue, U., Conley, T., & Trappe, S. (2012). Skeletal muscle plasticity with marathon training in novice runners. *Scandinavian Journal of Medicine & Science in Sports*, **22**(5), 662–670.

Lundberg, T. R., Fernandez-Gonzalo, R., Gustafsson, T., & Tesch, P. A. (2013). Aerobic exercise does not compromise muscle hypertrophy response to short-term resistance training. *Journal of Applied Physiology*, **114**(1), 81–89.

Marshall, R. N., Smeuninx, B., Seabright, A. P., Morgan, P. T., Atherton, P. J., Philp, A., & Breen, L. (2022). No effect of five days of bed rest or short-term resistance exercise prehabilitation on markers of skeletal muscle mitochondrial content and dynamics in older adults. *Physiological Reports*, **10**(13), e15345.

Martin, M. (2011). Cutadapt removes adapter sequences from high-throughput sequencing reads. *European Molecular Biology network Journal*, **17**(1), 10–12.

Martino, G., Valli, G., Sarto, F., Franchi, M. V., Narici, M. V., & De Vito, G. (2024). Neuromodulatory contribution to muscle force production after short-term unloading and active recovery. *Medicine and Science in Sports and Exercise*, **56**(9), 1830–1839.

Mendez, J. & Keys, A. (1960). Density and composition of mammalian muscle. *Metabolism*, **9**, 184–188.

Mikines, K. J., Richter, E. A., Dela, F., & Galbo, H. (1991). Seven days of bed rest decrease insulin action on glucose uptake in leg and whole body. *Journal of Applied Physiology (1985)*, **70**(3), 1245–1254.

Miotto, P. M., Mcglory, C., Bahniwal, R., Kamal, M., Phillips, S. M., & Holloway, G. P. (2019). Supplementation with dietary ω-3 mitigates immobilization-induced reductions in skeletal muscle mitochondrial respiration in young women. *Federation of American Societies for Experimental Biology Journal*, **33**(7), 8232–8240.

Monti, E., Franchi, M. V., Badiali, F., Quinlan, J. I., Longo, S., & Narici, M. V.(2020). The time-course of changes in muscle mass, architecture and power during 6 weeks of plyometric training. *Frontiers in Physiology*, **11**, 946.

Monti, E., Reggiani, C., Franchi, M. V., Toniolo, L., Sandri, M., Armani, A., Zampieri, S., Giacomello, E., Sarto, F., Sirago, G., Murgia, M., Nogara, L., Marcucci, L., Ciciliot, S., Šimunic, B., Pišot, R., & Narici, M. V. (2021). Neuro-muscular junction instability and altered intracellular calcium handling as early determinants of force loss during unloading in humans. *The Journal of Physiology*, **599**(12), 3037–3061.

Murgia, M., Nogara, L., Baraldo, M., Reggiani, C., Mann, M., & Schiaffino, S. (2021). Protein profile of fiber types in human skeletal muscle: A single-fiber proteomics study. *The Journal of Skeletal Muscle*, **11**(1), 24.

Murgia, M., Toniolo, L., Nagaraj, N., Ciciliot, S., Vindigni, V., Schiaffino, S., Reggiani, C., & Mann, M. (2017). Single muscle fiber proteomics reveals fiber-type-specific features of human muscle aging. *Cell Reports*, **19**(11), 2396–2409.

Murray, B., & Rosenbloom, C. (2018). Fundamentals of glycogen metabolism for coaches and athletes. *Nutrition Reviews*, **76**(4), 243.

Narici, M., De Vito, G., Franchi, M., Paoli, A., Moro, T., Marcolin, G., Grassi, B., Baldassarre, G., Zuccarelli, L., Biolo, G., di Girolamo, F. G., Fiotti, N., Dela, F., Greenhaff, P., & Maganaris, C. (2020). Impact of sedentarism due to the COVID-19 home confinement on neuromuscular, cardiovascular and metabolic health: Physiological and pathophysiological implications and recommendations for physical and nutritional countermeasures. *European Journal of Sport Science*, **21**(4), 614–635.

Neuhoff, V., Arold, N., Taube, D., & Ehrhardt, W. (1988). Improved staining of proteins in polyacrylamide gels including isoelectric focusing gels with clear background at nanogram sensitivity using Coomassie Brilliant Blue G-250 and R-250. *Electrophoresis*, **9**(6), 255–262.

Nunes, E. A., Stokes, T., McKendry, J., Currier, B. S., & Phillips, S. M. (2022). Disuse-induced skeletal muscle atrophy in disease and nondisease states in humans: Mechanisms, prevention, and recovery strategies. *American Journal of Physiology-Cell Physiology*, **322**(6), C1068–C1084.

Oikawa, S. Y., Holloway, T. M., & Phillips, S. M. (2019). The impact of step reduction on muscle health in aging: Protein and exercise as countermeasures. *Frontiers in Nutrition*, **6**, 75.

Phillips, B. E., Williams, J. P., Gustafsson, T., Bouchard, C., Rankinen, T., Knudsen, S., Smith, K., Timmons, J. A., & Atherton, P. J. (2013). Molecular networks of human muscle adaptation to exercise and age. *PLoS Genetics*, **9**(3), e1003389.

Pileggi, C. A., Hedges, C. P., D'Souza, R. F., Durainayagam, B. R., Zeng, N., Figueiredo, V. C., Hickey, A. J. R., Mitchell, C. J., & Cameron-Smith, D. (2023). Minimal adaptation of the molecular regulators of mitochondrial dynamics in response to unilateral limb immobilisation and retraining in middle-aged men. *European Journal of Applied Physiology*, **123**(2), 249–260.

Pillon, N. J., Gabriel, B. M., Dollet, L., Smith, J. A. B., Sardón Puig, L., Botella, J., Bishop, D. J., Krook, A., & Zierath, J. R. (2020). Transcriptomic profiling of skeletal muscle adaptations to exercise and inactivity. *Nature Communications*, **11**(1), 1–15.

Pišot, R., Marusic, U., Biolo, G., Mazzucco, S., Lazzer, S., Grassi, B., Reggiani, C., Toniolo, L., Di Prampero, P. E., Passaro, A., Narici, M., Mohammed, S., Rittweger, J., Gasparini, M., Gabrijelčič Blenkuš, M., & Šimunič, B. (2016). Greater loss in muscle mass and function but smaller metabolic alterations in older compared with younger men following 2 wk of bed rest and recovery. *Journal of Applied Physiology (1985)*, **120**(8), 922–929.

Popov, D. V., Makhnovskii, P. A., Zgoda, V. G., Gazizova, G. R., Vepkhvadze, T. F., Lednev, E. M., Motanova, E. S., Lysenko, E. A., Orlov, O. I., & Tomilovskaya, E. S. (2023). Rapid changes in transcriptomic profile and mitochondrial function in human soleus muscle after 3-day dry immersion. *Journal of Applied Physiology (1985)*, **134**(5), 1256–1264.

Powers, S. K., Wiggs, M. P., Duarte, J. A., Zergeroglu, A. M., & Demirel, H. A. (2012). Mitochondrial signaling contributes to disuse muscle atrophy. *American Journal of Physiology-Endocrinology and Metabolism*, **303**(1), E31–E39.

Preobrazenski, N., Seigel, J., Halliday, S., Janssen, I., & McGlory, C. (2023). Single-leg disuse decreases skeletal muscle strength, size, and power in uninjured adults: A systematic review and meta-analysis. *Journal of Cachexia, Sarcopenia and Muscle*, **14**(2), 684–696.

Quinlan, J. I., Franchi, M. V., Gharahdaghi, N., Badiali, F., Francis, S., Hale, A., Phillips, B. E., Szewczyk, N., Greenhaff, P. L., Smith, K., Maganaris, C., Atherton, P. J., & Narici, M. V. (2021). Muscle and tendon adaptations to moderate load eccentric vs. concentric resistance exercise in young and older males. *GeroScience*, **2021** 1–18.

Reidy, P. T., Lindsay, C. C., McKenzie, A. I., Fry, C. S., Supiano, M. A., Marcus, R. L., LaStayo, P. C., & Drummond, M. J. (2018). Aging-related effects of bed rest followed by eccentric exercise rehabilitation on skeletal muscle macrophages and insulin sensitivity. *Experimental Gerontology*, **107**, 37–49.

Roach, R. E. J., Cannegieter, S. C., & Lijfering, W. M. (2014). Differential risks in men and women for first and recurrent venous thrombosis: The role of genes and environment. *Journal of Thrombosis and Haemostasis*, **12**(10), 1593–1600.

Robinson, M. D., McCarthy, D. J., & Smyth, G. K. (2010). edgeR: A Bioconductor package for differential expression analysis of digital gene expression data. *Bioinformatics*, **26**(1), 139–140.

Rutter, J., Winge, D. R., & Schiffman, J. D. (2010). Succinate dehydrogenase – Assembly, regulation and role in human disease. *Mitochondrion*, **10**(4), 393–401.

Saltin, B., Blomqvist, G., Mitchell, J. H., Johnson, R. L., Wildenthal, K., & Chapman, C. B. (1968). Response to exercise after bed rest and after training. *Circulation*, **38**(Suppl 5), VII1–VII78.

Sarto, F., Spörri, J., Fitze, D. P., Quinlan, J. I., Narici, M. V., & Franchi, M. V. (2021). Implementing ultrasound imaging for the assessment of muscle and tendon properties in elite sports: Practical aspects, methodological considerations and future directions. *Sports Medicine*, **51**(6), 1–20.

Sarto, F., Stashuk, D. W., Franchi, M. V., Monti, E., Zampieri, S., Valli, G., Sirago, G., Candia, J., Hartnell, L. M., Paganini, M., Mcphee, J. S., De Vito, G., Ferrucci, L., Reggiani, C., & Narici, M. V. (2022). Effects of short-term unloading and active recovery on human motor unit properties, neuromuscular junction transmission and transcriptomic profile. *The Journal of Physiology*, **600**(21), 4731–4751.

Schiaffino, S., Gorza, L., Sartore, S., Saggin, L., Ausoni, S., Vianello, M., Gundersen, K., & LØmo, T. (1989). Three Myosin Heavy Chain isoforms in type 2 skeletal muscle fibres. *Journal of Muscle Research and Cell Motility*, **10**(3), 197–205.

Schindelin, J., Arganda-Carreras, I., Frise, E., Kaynig, V., Longair, M., Pietzsch, T., Preibisch, S., Rueden, C., Saalfeld, S., Schmid, B., Tinevez, J. Y., White, D. J., Hartenstein, V., Eliceiri, K., Tomancak, P., & Cardona, A. (2012). Fiji: An open-source platform for biological-image analysis. *Nature Methods*, **9**(7), 676–682.

Schoenfeld, B. J., Grgic, J., Haun, C., Itagaki, T., & Helms, E. R. (2019). Calculating set-volume for the limb muscles with the performance of multi-joint exercises: Implications for resistance training prescription. *Sports*, **7**(7), 177.

Sebastián, D., Sorianello, E., Segalés, J., Irazoki, A., Ruiz-Bonilla, V., Sala, D., Planet, E., Berenguer-Llergo, A., Muñoz, J. P., Sánchez-Feutrie, M., Plana, N., Hernández-Álvarez, M. I., Serrano, A. L., Palacín, M., & Zorzano, A. (2016). Mfn2 deficiency links age-related sarcopenia and impaired autophagy to activation of an adaptive mitophagy pathway. *European Molecular Biology Organization Journal*, **35**(15), 1677–1693.

Seynnes, O. R., Maganaris, C. N., de Boer, M. D., di Prampero, P. E., & Narici, M. V. (2008). Early structural adaptations to unloading in the human calf muscles. *Acta Physiologica*, **193**(3), 265–274.

Sharlo, K., Tyganov, S. A., Tomilovskaya, E., Popov, D. V., Saveko, A. A., & Shenkman, B. S. (2021). Effects of various muscle disuse states and countermeasures on muscle molecular signaling. *International Journal of Molecular Sciences*, **23**(1), 468.

Shenkman, B. S. (2016). From slow to fast: Hypogravity-induced remodeling of muscle fiber myosin phenotype. *Acta Naturae*, **8**(4), 47.

Shepherd, S. O., Cocks, M., Tipton, K. D., Witard, O. C., Ranasinghe, A. M., Barker, T. A., Wagenmakers, A. J. M., & Shaw, C. S. (2014). Resistance training increases skeletal muscle oxidative capacity and net intramuscular triglyceride breakdown in type I and II fibres of sedentary males. *Experimental Physiology*, **99**(6), 894–908.

Shiose, K., Takahashi, H., & Yamada, Y. (2022). Muscle glycogen assessment and relationship with body hydration status: A narrative review. *Nutrients*, **15**(1), 155.

Shiose, K., Yamada, Y., Motonaga, K., Sagayama, H., Higaki, Y., Tanaka, H., & Takahashi, H. (2016). Segmental extracellular and intracellular water distribution and muscle glycogen after 72-h carbohydrate loading using spectroscopic techniques. *Journal of Applied Physiology*, **121**(1), 205–211.

Shiose, K., Yamada, Y., Motonaga, K., & Takahashi, H. (2018). Muscle glycogen depletion does not alter segmental extracellular and intracellular water distribution measured using bioimpedance spectroscopy. *Journal of Applied Physiology*, **124**(6), 1420–1425.

Shur, N. F., Simpson, E. J., Crossland, H., Chivaka, P. K., Constantin, D., Cordon, S. M., Constantin-Teodosiu, D., Stephens, F. B., Lobo, D. N., Szewczyk, N., Narici, M., Prats, C., Macdonald, I. A., & Greenhaff, P. L. (2022). Human adaptation to immobilization: Novel insights of impacts on glucose disposal and fuel utilization. *Journal of Cachexia, Sarcopenia and Muscle*, **13**(6), 2999–3013.

Sirago, G., Candia, J., Franchi, M. V., Sarto, F., Monti, E., Toniolo, L., Reggiani, C., Giacomello, E., Zampieri, S., Hartnell, L. M., De Vito, G., Sandri, M., Ferrucci, L., & Narici, M. V. (2023). Upregulation of sarcolemmal hemichannels and inflammatory transcripts with neuromuscular junction instability during lower limb unloading in humans. *Biology (Basel)*, **12**, 431.

Slavin, M. B., Memme, J. M., Oliveira, A. N., Moradi, N., & Hood, D. A. (2022). Regulatory networks coordinating mitochondrial quality control in skeletal muscle. *American Journal of Physiology-Cell Physiology*, **322**(5), C913–C926.

Smerdu, V., Karsch-Mizrachi, I., Campione, M., Leinwand, L., & Schiaffino, S. (1994). Type IIx Myosin Heavy Chain transcripts are expressed in type IIb fibers of human skeletal muscle. *American Journal of Physiology*, **267**(6), C1723–C1728.

Smyth, G. K. (2004). Linear models and empirical bayes methods for assessing differential expression in microarray experiments. *Statistical Applications in Genetics and Molecular Biology*, **3**(1), 1–25.

Stein, T. P., & Bolster, D. R. (2006). Insights into muscle atrophy and recovery pathway based on genetic models. *Current Opinion in Clinical Nutrition and Metabolic Care*, **9**(4), 395–402.

Stokes, T., Timmons, J. A., Crossland, H., Tripp, T. R., Murphy, K., McGlory, C., Mitchell, C. J., Oikawa, S. Y., Morton, R. W., Phillips, B. E., Baker, S. K., Atherton, P. J., Wahlestedt, C., & Phillips, S. M. (2020). Molecular transducers of human skeletal muscle remodeling under different loading states. *Cell Reports*, **32**(5), 107980.

Stuart, C. A., Shangraw, R. E., Prince, M. J., Peters, E. J., & Wolfe, R. R. (1988). Bed-rest-induced insulin resistance occurs primarily in muscle. *Metabolism*, **37**(8), 802–806.

Suetta, C., Frandsen, U., Jensen, L., Jensen, M. M., Jespersen, J. G., Hvid, L. G., Bayer, M., Petersson, S. J., Schrøder, H. D., Andersen, J. L., Heinemeier, K. M., Aagaard, P., Schjerling, P., & Kjaer, M. (2012). Aging affects the transcriptional regulation of human skeletal muscle disuse atrophy. *PLoS ONE*, **7**(12), e51238.

Suetta, C., Hvid, L. G., Justesen, L., Christensen, U., Neergaard, K., Simonsen, L., Ortenblad, N., Magnusson, S. P., Kjaer, M., & Aagaard, P. (2009). Effects of aging on human skeletal muscle after immobilization and retraining. *Journal of Applied Physiology (1985)*, **107**(4), 1172–1180.

Tesch, P. A., Colliander, E. B., & Kaiser, P. (1986). Muscle metabolism during intense, heavy-resistance exercise. *European Journal of Applied Physiology and Occupational Physiology*, **55**(4), 362–366.

Tesch, P. A., Fernandez-Gonzalo, R., & Lundberg, T. R. (2017). Clinical applications of iso-inertial, eccentric-overload (YoYo^{TM}) resistance exercise. *Frontiers in Physiology*, **8**, 241.

Tesch, P. A., Lundberg, T. R., & Fernandez-Gonzalo, R. (2016). Unilateral lower limb suspension: From subject selection to "omic" responses. *Journal of Applied Physiology*, **120**(10), 1207–1214.

Tesch, P. A., Ploutz-Snyder, L. L., Yström, L., Castro, M. J., & Dudley, G. A. (1998). Skeletal muscle glycogen loss evoked by resistance exercise. *Journal of Strength and Conditioning Research*. **12**(2), 67–73

Timmons, J. A., Norrbom, J., Schéele, C., Thonberg, H., Wahlestedt, C., & Tesch, P. (2006). Expression profiling following local muscle inactivity in humans provides new perspective on diabetes-related genes. *Genomics*, **87**(1), 165–172.

Tracy, B. L., Ivey, F. M., Jeffrey Metter, E., Fleg, J. L., Siegel, E. L., & Hurley, B. F. (2003). A more efficient magnetic resonance imaging-based strategy for measuring quadriceps muscle volume. *Medicine and Science in Sports and Exercise*, **35**(3), 425–433.

Trappe, S., Harber, M., Creer, A., Gallagher, P., Slivka, D., Minchev, K., & Whitsett, D. (2006). Single muscle fiber adaptations with marathon training. *Journal of Applied Physiology (1985)*, **101**(3), 721–727.

Valli, G., Sarto, F., Casolo, A., Del, V. A., Franchi, M. V., Narici, M. V., & De, V. G. (2023). Lower limb suspension induces threshold-specific alterations of motor units properties that are reversed by active recovery. *Journal of Sport and Health Science*, **13**(2), 264–276.

Vinel, C., Lukjanenko, L., Batut, A., Deleruyelle, S., Pradère, J.-P., Le Gonidec, S., Dortignac, A., Geoffre, N., Pereira, O., Karaz, S., Lee, U., Camus, M., Chaoui, K., Mouisel, E., Bigot, A., Mouly, V., Vigneau, M., Pagano, A. F., Chopard, A., … Dray, C. (2018). The exerkine apelin reverses age-associated sarcopenia. *Nature Medicine*, **24**(9), 1360–1371.

Wall, B. T., Dirks, M. L., Snijders, T., Senden, J. M. G., Dolmans, J., & van Loon, L. J. C. (2013). Substantial skeletal muscle loss occurs during only 5 days of disuse. *Acta Physiologica (Oxford)*, **210**(3), 600–611.

Wang, L., Wang, S., & Li, W. (2012). RSeQC: Quality control of RNA-seq experiments. *Bioinformatics*, **28**(16), 2184–2185.

Wernbom, M., Augustsson, J., & Thomeé, R. (2007). The influence of frequency, intensity, volume and mode of strength training on whole muscle cross-sectional area in humans. *Sports Medicine (Auckland, New Zealand)*, **37**(3), 225–264.

Wood, D. E., & Salzberg, S. L. (2014). Kraken: Ultrafast metagenomic sequence classification using exact alignments. *Genome Biology*, **15**(3), 1–12.

Zachwieja, J. J., Costill, D. L., Pascoe, D. D., Robergs, R. A., & Fink, W. J. (1991). Influence of muscle glycogen depletion on the rate of resynthesis. *Medicine and Science in Sports and Exercise*, **23**(1), 44–48.

Zuccarelli, L., Baldassarre, G., Magnesa, B., Degano, C., Comelli, M., Gasparini, M., Manferdelli, G., Marzorati, M., Mavelli, I., Pilotto, A., Porcelli, S., Rasica, L., Šimunič, B., Pišot, R., Narici, M., & Grassi, B. (2021). Peripheral impairments of oxidative metabolism after a 10-day bed rest are upstream of mitochondrial respiration. *The Journal of Physiology*, **599**(21), 4813–4829.

Additional information

Data availability statement

RNA-seq datasets are available at the Gene Expression Omnibus repository: https://www.ncbi.nlm.nih.gov/geo/query/acc.cgi?acc=GSE211204. Other data supporting the findings of this study will be made available from the corresponding author upon reasonable request.

Competing interests

None declared.

Author contributions

M.V.F., G.D.V., L.F. and M.V.N. contributed to the conception or design of the work. M.V.F., F.S., G.S., G.V., M.P. and T.M. contributed to the data acquisition. M.V.F., J.C., F.S., G.V., L.H., E.G., L.T., E.M., L.N., T.M., L.B. and M.A.P. contributed to the data analysis. M.V.F., J.C., F.S., E.M., L.B., M.A.P., B.G., R.B., G.D.V., L.F. and M.V.N. contributed to the data interpretation. M.V.F. and M.V.N. drafted the manuscript. M.V.F., J.C., F.S., G.S., G.V., E.M., M.M., L.B., M.A.P., B.G., R.B., G.D.V., L.F. and M.V.N. revised the manuscript critically for important intellectual content. All authors approved the final version of the manuscript, agreed to be accountable for all aspects of the work in ensuring that questions related to the accuracy or integrity of any part of the work are appropriately investigated and resolved; and all persons designated as authors qualify for authorship, and all those who qualify for authorship are listed.

Funding

The present study was funded by the Italian Space Agency (ASI), MARcatori biologici e funzionali per la biomeccanica aStronautica di PREcisione – MARS-PRE, Project n. DC-VUM-2017-006 (funding received by M.V.N.), by the NextGenerationEU/Italian Ministry of University and Research (MUR) PRIN 2022 PNRR, ReActiveAge, Project no. P2022FNCPR (funding received by M.V.F.), by the PRIN project 'NeuAge' (n.2017CBF8NJ_001) (funding received by M.V.N. and M.A.P.) and by PRIN project 'InactivAge' (no. 2020EM9A8X) (funding received by R.B. and M.V.N.). The authors are grateful to ASI and EU/MUR for granting these funds to allow all the experiments to be performed. This work was also partially funded by the Intramural Research Program of the National Institute on Aging (Baltimore, MD, USA) of the National Institutes of Health (funding received by L.F.).

Acknowledgements

The authors would like to thank Dr Giovanni Martino for valuable suggestions on the manuscript, Dr Sandra Zampieri for supervising the process for producing cryosections, Dr Martina Baraldo for help during muscle biopsy immunofluorescence analyses and Mr Paul Ritsche for assistance during ultrasound data collection and the training sessions.

Open access publishing facilitated by Universita degli Studi di Padova, as part of the Wiley - CRUI-CARE agreement.

Keywords

exercise physiology, gene expression, muscle adaptation, muscle atrophy, muscle physiology, muscle plasticity, resistance training, unloading responses

Supporting information

Additional supporting information can be found online in the Supporting Information section at the end of the HTML view of the article. Supporting information files available:

Peer Review History